

# Asymptotic Analysis of Complex LASSO via Complex Approximate Message Passing (CAMP)

Arian Maleki, Laura Anitori, *Student Member, IEEE*, Zai Yang, and Richard G. Baraniuk, *Fellow, IEEE*

**Abstract**—Recovering a sparse signal from an undersampled set of random linear measurements is the main problem of interest in compressed sensing. In this paper, we consider the case where both the signal and the measurements are complex-valued. We study the popular recovery method of  $\ell_1$ -regularized least squares or LASSO. While several studies have shown that LASSO provides desirable solutions under certain conditions, the precise asymptotic performance of this algorithm in the complex setting is not yet known. In this paper, we extend the approximate message passing (AMP) algorithm to solve the complex-valued LASSO problem and obtain the complex approximate message passing algorithm (CAMP). We then generalize the state evolution framework recently introduced for the analysis of AMP to the complex setting. Using the state evolution, we derive accurate formulas for the phase transition and noise sensitivity of both LASSO and CAMP. Our theoretical results are concerned with the case of i.i.d. Gaussian sensing matrices. Simulations confirm that our results hold for a larger class of random matrices.

**Index Terms**—Approximate message passing (AMP), complex-valued LASSO, compressed sensing (CS), minimax analysis.

## I. INTRODUCTION

RECOVERING a sparse signal from an undersampled set of random linear measurements is the main problem of interest in compressed sensing (CS). In the past few years, many algorithms have been proposed for signal recovery, and their performance has been analyzed both analytically and empirically [1]–[6]. However, whereas most of the theoretical work has focused on the case of real-valued signals and measurements, in many applications, such as magnetic resonance imaging and radar, the signals are more easily representable in the complex domain [7]–[10]. In such applications, the real and

Manuscript received August 01, 2011; revised August 25, 2012; accepted October 20, 2012. Date of publication March 12, 2013; date of current version June 12, 2013. This work was supported in part by the Grants NSF CCF-0431150, CCF-0926127, and CCF-1117939, DARPA/ONR N66001-11-C-4092 and N66001-11-1-4090, ONR N00014-08-1-1112, N00014-10-1-0989, and N00014-11-1-0714, AFOSR FA9550-09-1-0432, ARO MURI W911NF-07-1-0185, and W911NF-09-1-0383, and in part by the TI Leadership University Program.

A. Maleki is with the Department of Statistics, Columbia University, New York, NY 10027 USA (e-mail: arian.maleki@rice.edu).

L. Anitori is with TNO, NL-2509 JG The Hague, The Netherlands (e-mail: laura.anitori@tno.nl).

Z. Yang is with the Exquisitus, Center for E-City, School of Electrical and Electronic Engineering, Nanyang Technological University, Singapore 639798 (e-mail: yang0248@e.ntu.edu.sg).

R. Baraniuk is with the Department of Electrical and Computer Engineering, Rice University, Houston, TX 77251 USA (e-mail: richb@rice.edu).

Communicated by M. Elad, Associate Editor for Signal Processing.

Color versions of one or more of the figures in this paper are available online at <http://ieeexplore.ieee.org>.

Digital Object Identifier 10.1109/TIT.2013.2252232

imaginary components of a complex signal are often either zero or nonzero simultaneously. Therefore, recovery algorithms may benefit from this prior knowledge. Indeed, the results presented in this paper confirm this intuition.

Motivated by this observation, we investigate the performance of the complex-valued LASSO in the case of noise-free and noisy measurements. The derivations are based on the state evolution (SE) framework, presented previously in [3]. Also a new algorithm, complex approximate message passing (CAMP), is presented to solve the complex LASSO problem. This algorithm is an extension of the AMP algorithm [3], [11]. However, the extension of AMP and its analysis from the real to the complex setting is not trivial; although CAMP shares some interesting features with AMP, it is substantially more challenging to establish the characteristics of CAMP. Furthermore, some important features of CAMP are specific to complex-valued signals and the relevant optimization problem. Note that the extension of the Bayesian-AMP algorithm to complex-valued signals has been considered elsewhere [12], [13] and is not the main focus of this work.

In the next section, we briefly review some of the existing algorithms for sparse signal recovery in the real-valued setting and then focus on recovery algorithms for the complex case, with particular attention to the AMP and CAMP algorithms. We then introduce two criteria that we use as measures of performance for various algorithms in noiseless and noisy settings. Based on these criteria, we establish the novelty of our results compared to the existing work. An overview of the organization of the rest of the paper is provided in Section I-G.

### A. Real-Valued Sparse Recovery Algorithms

Consider the problem of recovering a sparse vector  $s_o \in \mathbb{R}^N$  from a noisy undersampled set of linear measurements  $y \in \mathbb{R}^n$ , where  $y = As_o + w$  and  $w$  is the noise. Let  $k$  denote the number of nonzero elements of  $s_o$ . The measurement matrix  $A$  has i.i.d. elements from a given distribution on  $\mathbb{R}$ . Given  $y$  and  $A$ , we seek an approximation to  $s_o$ .

Many recovery algorithms have been proposed, ranging from convex relaxation techniques to greedy approaches to iterative thresholding schemes. See [1] and the references therein for an exhaustive list of algorithms. Maleki and Donoho [6] have compared several different recovery algorithms and concluded that among the algorithms compared in that paper, the  $\ell_1$ -regularized least squares, a.k.a. LASSO or BPDN [2], [14] that seeks the minimizer of  $\min_x \frac{1}{2} \|y - Ax\|_2^2 + \lambda \|x\|_1$ , provides the best performance in the sense of the sparsity/measurement tradeoff. Recently, several iterative thresholding algorithms have been

proposed for solving LASSO using few computations per-iteration; this enables the use of the LASSO in high-dimensional problems. See [15] and the references therein for an exhaustive list of these algorithms.

In this paper, we are particularly interested in AMP [3]. Starting from  $x^0 = 0$  and  $z^0 = y$ , AMP uses the following iterations:

$$\begin{aligned} x^{t+1} &= \eta_o(x^t + A^T z^t; \tau_t) \\ z^t &= y - Ax^t + \frac{|I^t|}{n} z^{t-1} \end{aligned}$$

where  $\eta_o(x; \tau) = (|x| - \tau)_+ \text{sign}(x)$  is the soft thresholding function,  $\tau_t$  is the threshold parameter, and  $I^t$  is the active set of  $x^t$ , i.e.,  $I^t = \{i \mid x_i^t \neq 0\}$ . The notation  $|I^t|$  denotes the cardinality of  $I^t$ . As we will describe later, the strong connection between AMP and LASSO and the ease of predicting the performance of AMP has led to an accurate performance analysis of LASSO [11], [16].

### B. Complex-Valued Sparse Recovery Algorithms

Consider the complex setting, where the signal  $s_o$ , the measurements  $y$ , and the matrix  $A$  are complex-valued. The success of LASSO has motivated researchers to use similar techniques in this setting as well. We consider the following two schemes that have been used in the signal processing literature.

1) r-LASSO: The simplest extension of the LASSO to the complex setting is to consider the complex signal and measurements as a  $2N$ -dimensional real-valued signal and  $2n$ -dimensional real-valued measurements, respectively. Let the superscripts  $R$  and  $I$  denote the real and imaginary parts of a complex number, respectively. Define  $\tilde{y} \stackrel{\Delta}{=} [(y^R)^T, (y^I)^T]^T$  and  $\tilde{s}_o \stackrel{\Delta}{=} [(s_o^R)^T, (s_o^I)^T]^T$ , where the superscript  $T$  denotes the transpose operator. We have

$$\tilde{y} = \underbrace{\begin{pmatrix} A^R & -A^I \\ A^I & A^R \end{pmatrix}}_{\tilde{A} \stackrel{\Delta}{=}} \tilde{s}_o.$$

We then search for an approximation of  $\tilde{s}_o$  by solving  $\arg \min_{\tilde{x}} \frac{1}{2} \|\tilde{y} - \tilde{A}\tilde{x}\|_2^2 + \lambda \|\tilde{x}\|_1$  [17], [18]. We call this algorithm r-LASSO. The limit of the solution as  $\lambda \rightarrow 0$  is

$$\arg \min_{\tilde{x}} \|\tilde{x}\|_1, \text{ s.t. } \tilde{y} = \tilde{A}\tilde{x}$$

which is called the basis pursuit problem, or r-BP in this paper. It is straightforward to extend the analyses of LASSO and BP for the real-valued signals to r-LASSO and r-BP.<sup>1</sup>

r-LASSO ignores the information about any potential grouping of the real and imaginary parts. But, in many applications, the real and imaginary components tend to be either zero or nonzero simultaneously. Considering this

<sup>1</sup>The asymptotic theoretical results on LASSO and BP consider i.i.d. Gaussian measurement matrices [19]. However, it has been conjectured that the results are universal and hold for a “larger” class of random matrices [11], [20].

extra information in the recovery stage may improve the overall performance of a CS system.

2) c-LASSO: Another natural extension of the LASSO to the complex setting is the following optimization problem that we term c-LASSO

$$\min \frac{1}{2} \|y - Ax\|_2^2 + \lambda \|x\|_1$$

where the complex  $\ell_1$ -norm is defined as  $\|x\|_1 \stackrel{\Delta}{=} \sum_i |x_i| = \sum_i \sqrt{(x_i^R)^2 + (x_i^I)^2}$  [4], [5], [21]–[23]. The limit of the solution as  $\lambda \rightarrow 0$  is

$$\arg \min_x \|x\|_1, \text{ s.t. } y = Ax$$

which we refer to as c-BP.

An important question we address in this paper is: Can we measure how much the grouping of the real and the imaginary parts improves the performance of c-LASSO compared to r-LASSO? Several papers have considered similar problems [24]–[41] and have provided guarantees on the performance of c-LASSO. However, the results are usually inconclusive because of the loose constants involved in the analyses. This paper addresses the above questions with an analysis that does not involve any loose constants and therefore provides accurate comparisons.

Motivated by the recent results in the asymptotic analysis of the LASSO [3], [11], we first derive the CAMP algorithm as a fast and efficient algorithm for solving the c-LASSO problem. We then extend the SE framework introduced in [3] to predict the performance of the CAMP algorithm in the asymptotic setting. Since the CAMP algorithm solves c-LASSO, such predictions are accurate for c-LASSO as well for  $N \rightarrow \infty$ . The analysis carried out in this paper provides new information and insight on the performance of the c-LASSO that was not known before such as the least favorable distribution and the noise sensitivity of c-LASSO and CAMP. A more detailed description of the contributions of this paper is summarized in Section I-E.

### C. Notation

Let  $|\alpha|$ ,  $\angle \alpha$ ,  $\alpha^*$ ,  $\mathcal{R}(\alpha)$ , and  $\mathcal{I}(\alpha)$  denote the amplitude, phase, conjugate, real part, and imaginary part of  $\alpha \in \mathbb{C}$ , respectively. Furthermore, for the matrix  $A \in \mathbb{C}^{n \times N}$ ,  $A^*$ ,  $A_\ell$ , and  $A_{\ell j}$  denote the conjugate transpose,  $\ell^{\text{th}}$  column, and  $\ell j^{\text{th}}$  element of matrix  $A$ . We are interested in approximating a sparse signal  $s_o \in \mathbb{C}^N$  from an undersampled set of noisy linear measurements  $y = As_o + w$ .  $A \in \mathbb{C}^{n \times N}$  has i.i.d. random elements (with independent real and imaginary parts) from a given distribution that satisfies  $\mathbb{E} A_{\ell j} = 0$  and  $\mathbb{E} |A_{\ell j}|^2 = \frac{1}{n}$ , and  $w \in \mathbb{C}^N$  is the measurement noise. Throughout this paper, we assume that the noise is i.i.d.  $CN(0, \sigma^2)$ , where  $CN$  stands for the complex normal distribution.

We are interested in the asymptotic setting where  $\delta = n/N$  and  $\rho = k/n$  are fixed, while  $N \rightarrow \infty$ . We further assume that the elements of  $s_o$  are i.i.d.  $s_{o,i} \sim (1-\rho\delta)\delta_0(|s_{o,i}|) + \rho\delta G(s_{o,i})$ , where  $G$  is an unknown probability distribution with no point

mass at 0, and  $\delta_0$  is a Dirac delta function.<sup>2</sup> Clearly, the expected number of nonzero elements in the vector  $s_o$  is  $\rho\delta N$ . We call this value the *sparsity level* of the signal. In this model, we are assuming that all the nonzero real and imaginary coefficients are paired. This quantifies the maximum amount of improvement the c-LASSO gains by grouping the real and imaginary parts.

We use the notations  $\mathbb{E}$ ,  $\mathbb{E}_X$ , and  $\mathbb{E}_{X \sim F}$  for expected value, conditional expected value given the random variable  $X$ , and expected value with respect to a random variable  $X$  drawn from the distribution  $F$ , respectively. Define  $\mathcal{F}_{\epsilon,\gamma}$  as the family of distributions  $F$  with  $\mathbb{E}_{X \sim F}(\mathbb{I}(|X| = 0)) \geq 1 - \epsilon$  and  $\mathbb{E}_{X \sim F}(|X|^2) \leq \epsilon\gamma^2$ , where  $\mathbb{I}$  denotes the indicator function. An important distribution in this class is  $q_o(X) \stackrel{\Delta}{=} q(|X|) \stackrel{\Delta}{=} (1 - \epsilon)\delta_0(|X|) + \epsilon\delta_\gamma(|X|)$ , where  $\delta_\gamma(|X|) \stackrel{\Delta}{=} \delta_0(|X| - \gamma)$ . Note that this distribution is independent of the phase and in addition to a point mass at zero has another point mass at  $\gamma$ . Finally, define  $\mathcal{F}_\epsilon \stackrel{\Delta}{=} \{F \mid \mathbb{E}_{X \sim F}(\mathbb{I}(|X| \neq 0)) \leq \epsilon\}$ .

#### D. Performance Criteria

We compare c-LASSO with r-LASSO in both the noise-free and noisy measurements cases. For each scenario, we define a specific measure to compare the performance of the two algorithms.

*1) Noise-Free Measurements:* Consider the problem of recovering  $s_o$  drawn from  $s_{o,i} \stackrel{\text{i.i.d.}}{\sim} (1 - \rho\delta)\delta_0(|s_{o,i}|) + \rho\delta G(s_{o,i})$ , from a set of noise free measurements  $y = As_o$ . Let  $\mathcal{A}_\alpha$  be a sparse recovery algorithm with free parameter  $\alpha$ . For instance,  $\mathcal{A}$  may be the c-LASSO algorithm and the free parameter of the algorithm is the regularization argument  $\lambda$ . Given  $(y, A)$ ,  $\mathcal{A}_\alpha$  returns an estimate  $\hat{x}^{\mathcal{A}_\alpha}$  of  $s_o$ . Suppose that in the noise free case, as  $N \rightarrow \infty$ , the performance of  $\mathcal{A}_\alpha$  exhibits a sharp phase transition, i.e., for every value of  $\delta$ , there exists  $\rho^{\mathcal{A}_\alpha}(\delta)$ , below which  $\lim_{N \rightarrow \infty} \|\hat{x}^{\mathcal{A}_\alpha} - s_o\|^2/N \rightarrow 0$  almost surely, while for  $\rho > \rho^{\mathcal{A}_\alpha}(\delta)$ ,  $\mathcal{A}_\alpha$  fails and  $\lim_{N \rightarrow \infty} \|\hat{x}^{\mathcal{A}_\alpha} - s_o\|^2/N \not\rightarrow 0$ . The phase transition has been studied both empirically and theoretically for many sparse recovery algorithms [6], [19], [20], [42]–[45]. The phase transition curve  $\rho^{\mathcal{A}_\alpha}(\delta)$  specifies the fundamental exact recovery limit of algorithm  $\mathcal{A}_\alpha$ .

The free parameter  $\alpha$  can strongly affect the performance of the sparse recovery algorithm [6]. Therefore, optimal tuning of this parameter is essential in practical applications. One approach is to tune the parameter for the highest phase transition [6],<sup>3</sup> i.e.,

$$\rho^{\mathcal{A}}(\delta) \stackrel{\Delta}{=} \sup_{\alpha} \rho^{\mathcal{A}_\alpha}(\delta).$$

In other words,  $\rho^{\mathcal{A}}$  is the best performance  $\mathcal{A}_\alpha$  provides in the exact sparse signal recovery problem, if we know how to tune the algorithm properly. Based on this framework, we say algorithm  $\mathcal{A}$  *outperforms*  $\mathcal{B}$  at a given  $\delta$ , if and only if  $\rho^{\mathcal{A}}(\delta) > \rho^{\mathcal{B}}(\delta)$ .

<sup>2</sup>This assumption is not necessary and as long as the marginal distribution of  $s_o$  converges to a given distribution the statements of this paper hold. For further information on this, see [11] and [16].

<sup>3</sup>In this paper, we consider algorithms whose phase transitions do not depend on the distribution  $G$  of nonzero coefficients. Otherwise, one could use the max-min framework introduced in [6].

*2) Noisy Measurements:* Consider the problem of recovering  $s_o$  distributed according to  $s_{o,i} \stackrel{\text{i.i.d.}}{\sim} (1 - \rho\delta)\delta_0(|s_{o,i}|) + \rho\delta G(s_{o,i})$ , from a set of noisy linear observations  $y = As_o + w$  where  $w_i \stackrel{\text{i.i.d.}}{\sim} CN(0, \sigma^2)$ . In the presence of measurement noise, exact recovery is not possible. Therefore, tuning the parameter for the highest phase transition curve does not necessarily provide the optimal performance. In this section, we explain the *optimal noise sensitivity tuning* introduced in [11]. Consider the  $\ell_2$ -norm as a measure for the reconstruction error and assume that  $\frac{\|\hat{x}^{\mathcal{A}_\alpha} - s_o\|_2^2}{N} \rightarrow \text{MSE}(\rho, \delta, \alpha, \sigma, G)$  almost surely. Define the *noise sensitivity* of the algorithm  $\mathcal{A}_\alpha$  as

$$\text{NS}(\rho, \delta, \alpha) \stackrel{\Delta}{=} \sup_{\sigma > 0} \sup_G \frac{\text{MSE}(\rho, \delta, \alpha, \sigma, G)}{\sigma^2} \quad (1)$$

where  $\alpha$  denotes the tuning parameter of the algorithm  $\mathcal{A}_\alpha$ . If the noise sensitivity is large, then the measurement noise may severely degrade the final reconstruction. In (1) we search for the distribution that induces the maximum reconstruction error to the algorithm. This ensures that for other signal distributions, the reconstruction error is smaller. By tuning  $\alpha$ , we may obtain better estimate of  $s_o$ . Therefore, we tune the parameter  $\alpha$  to obtain the lowest noise sensitivity, i.e.,

$$\text{NS}(\rho, \delta) \stackrel{\Delta}{=} \inf_{\alpha} \text{NS}(\rho, \delta, \alpha).$$

Based on this framework, we say that algorithm  $\mathcal{A}$  outperforms  $\mathcal{B}$  at a given  $\delta$  and  $\rho$  if and only if  $\text{NS}^{\mathcal{A}}(\delta, \rho) < \text{NS}^{\mathcal{B}}(\delta, \rho)$ .

#### E. Contributions

In this paper, we first develop the CAMP algorithm that is a simple and fast converging iterative method for solving c-LASSO. We extend the SE, introduced recently as a framework for accurate asymptotic predictions of the AMP performance, to CAMP.<sup>4</sup> We will then use the connection between CAMP and c-LASSO to provide an accurate asymptotic analysis of the c-LASSO problem. We aim to characterize the phase transition curve (noise-free measurements) and noise sensitivity (noisy measurements) of c-LASSO and CAMP when the real and imaginary parts are paired, i.e., they are both zero or nonzero simultaneously. Both criteria have been extensively studied for the real signals (and hence for the r-LASSO) [3], [11]. The results of our predictions are summarized in Figs. 1–3. Fig. 1 compares the phase transition curve of c-BP and CAMP with the phase transition curve of r-BP. As we expected, c-BP outperforms r-BP since it exploits the connection between the real and imaginary parts. If  $\rho_{\text{SE}}(\delta)$  denotes the phase transition curve, then we also prove that  $\rho_{\text{SE}}(\delta) \sim \frac{1}{\log(1/\delta)}$  as  $\delta \rightarrow 0$ . Comparing this with  $\rho_{\text{SE}}^R(\delta) \sim \frac{1}{2\log(1/\delta)}$  for the r-LASSO [19], we conclude that

$$\lim_{\delta \rightarrow 0} \frac{\rho_{\text{SE}}(\delta)}{\rho_{\text{SE}}^R(\delta)} = 2.$$

<sup>4</sup>Note that SE has been proved to be accurate only for the case of Gaussian measurement matrices [16], [46]. But, extensive simulations have confirmed its accuracy for a large class of random measurement matrices [3], [11]. The results of our paper are also provably correct for complex Gaussian measurement matrices. But, our simulations confirm that they hold for broader set of matrices.

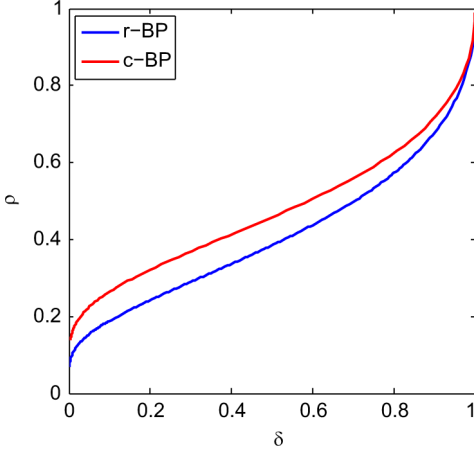


Fig. 1. Comparison of the phase transition curve of the r-BP and c-BP. When all the nonzero real and imaginary parts of the signal are grouped, the phase transition of c-BP outperforms that of r-BP.

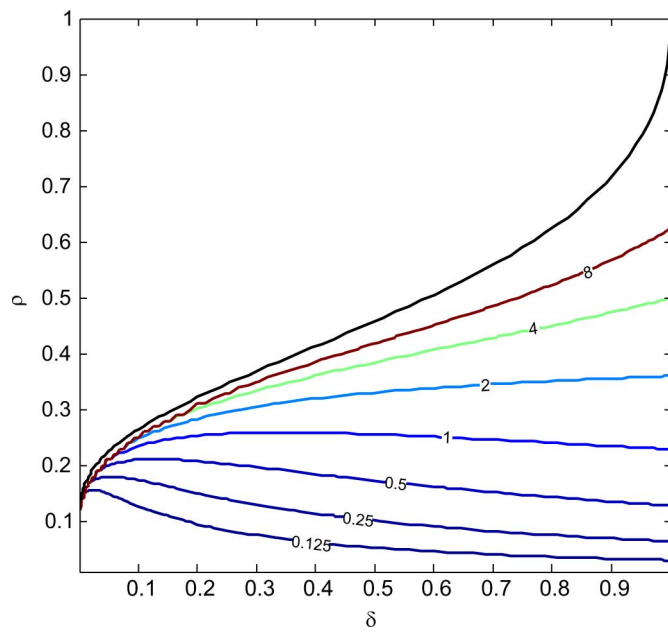


Fig. 2. Contour lines of noise sensitivity in the  $(\delta, \rho)$  plane. The black curve is the phase transition curve at which the noise sensitivity is infinite. The colored lines display the level sets of  $\text{NS}(\rho, \delta) = 0.125, 0.25, 0.5, 1, 2, 4, 8$ .

This means that, in the very high undersampling regime, the c-LASSO can recover signals that are two times more dense than the signals that are recovered by r-LASSO. Fig. 2 exhibits the noise sensitivity of c-LASSO and CAMP. We prove in Section III-C that, as the sparsity approaches the phase transition curve, the noise sensitivity grows up to infinity. Finally, Fig. 3 compares the contour plots of the noise sensitivity of c-LASSO with those of the r-LASSO. For the fixed value noise sensitivity, the level set of the c-LASSO is higher than that of r-LASSO. It is worth noting that the same comparisons hold between CAMP and AMP, as we will clarify in Section III-D.

#### F. Related Work

The SE framework used in this paper was first introduced in [3]. Deriving the phase transition and noise sensitivity of the LASSO for real-valued signals and real-valued measurements

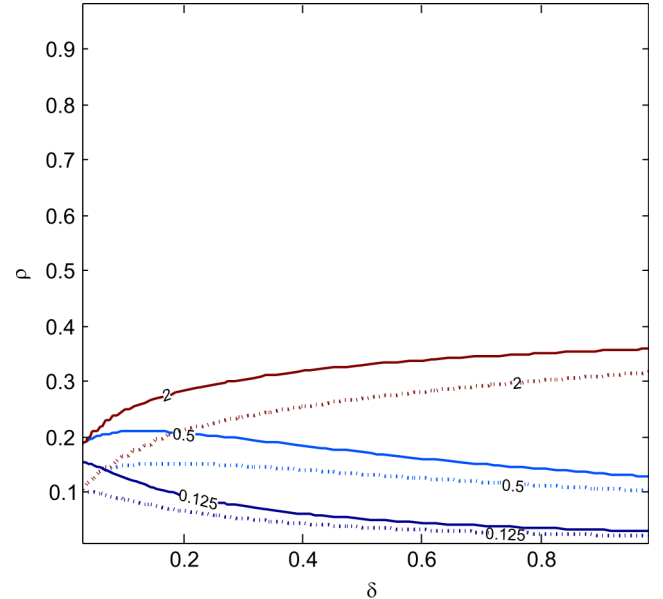


Fig. 3. Comparison of the noise sensitivity of r-LASSO with the noise sensitivity of c-LASSO. The colored solid lines present the level sets of the  $\text{NS}(\rho, \delta) = 0.125, 0.5, 2$  for the c-LASSO, and the colored dotted lines display the same level sets for the r-LASSO.

from SE is due to [11]; see [47] for more comprehensive discussion. Finally, the derivation of AMP from the full sum-product message passing is due to [48]. Our main contribution in this paper is to extend these results to the complex setting. Not only is the analysis of the SE more challenging in this setting, but it also provides new insights on the performance of c-LASSO that have not been available. For instance, the noise sensitivity of c-LASSO has not previously been determined.

The recovery of sparse complex signals is a special case of group sparsity or block sparsity, where all the groups are nonoverlapping and have size 2. According to the group sparsity assumption, the nonzero elements of the signal tend to occur in groups or clusters. One of the algorithms used in this context is the group-LASSO [35], [37]. Consider a signal  $s_o \in \mathbb{R}^N$ . Partition the indices of  $s_o$  into  $m$  groups  $g_1, \dots, g_m$ . The group-LASSO algorithm minimizes the following cost function:

$$\min_x \frac{1}{2} \|y - Ax\|_2^2 + \sum_{i=1}^m \lambda_i \|x_{g_i}\|_2 \quad (2)$$

where the  $\lambda_i$ 's are regularization parameters.

The group-Lasso algorithm has been extensively studied in the literature [24]–[41]. We briefly review several papers and emphasize the differences from our work. Bach [38] analyzes the consistency of the group LASSO estimator in the presence of noise. Fixing the signal  $s_o$ , it provides conditions under which the group LASSO is consistent as  $n \rightarrow \infty$ . In [39] and [49], the authors consider a weak notion of consistency, i.e., exact support recovery. However, Wainwright *et al.* [49] prove that in the setting we are interested in, i.e.,  $k/n = \rho$  and  $n/N = \delta$ , even exact support recovery is not possible. When noise is present, our goal is neither exact recovery nor exact support recovery. Instead, we characterize the mean square error (MSE) of the

reconstruction. This criterion has been considered in [24] and [40]. Although the results of [24] and [40] show qualitatively the benefit of group sparsity, they do not characterize the difference quantitatively. In fact, loose constants in both the error bound and the number of samples do not permit accurate performance comparison. In our analysis, no loose constant is involved, and we provide very accurate characterization of the MSE.

Group sparsity and group-LASSO are also of interest in the sparse recovery community. For example, the analysis carried out in [26], [29], and [30] is based on “coherence.” These results provide sufficient conditions with again loose constants as discussed above. The work of [31]–[33] addresses this issue by an accurate analysis of the algorithm in the noiseless setting  $\sigma = 0$ . They provide a very accurate estimate of the phase transition curve for the group-LASSO. However, SE provides a more flexible framework to analyze c-LASSO than the analysis of [33], and it provides more information than just the phase transition curve. For instance, it points to the least favorable distribution of the input and noise sensitivity of c-LASSO.

The Bayesian approach that assumes a hidden Markov model for the signal has also been explored for the recovery of group sparse signals [50], [51]. It has been shown that AMP combined with an expectation maximization algorithm (for estimating the parameters of the distribution) leads to promising results in practice [12]. Kamilov *et al.* [52] have taken the first step toward a theoretical understanding of such algorithms. However, the complete understanding of the expectation maximization employed in such methods is not available yet. Furthermore, the success of such algorithms seems to be dependent on the match between the assumed and actual prior distribution. Such dependences have not been theoretically analyzed yet. In this paper, we assume that the distribution of nonzero coefficients is not known beforehand and characterize the performance of c-LASSO for the least favorable distribution.

While writing this paper, we were made aware that in an independent work, Donoho *et al.* are extending the SE framework to the general setting of group sparsity [53]. Their work considers the SE framework for the group-LASSO problem and will include the generalization of the analysis provided in this paper to the case where the variables tend to cluster in groups of size  $B$ .

Both complex signals and group-sparse signals are special cases of model-based CS [54]. By introducing more structured models for the signal, Baraniuk *et al.* [54] prove that the number of measurements needed is proportional to the “complexity” of the model rather than the sparsity level [55]. The results in model-based CS also suffer from loose constants in both the number of measurements and the MSE bounds. Finally, from an algorithmic point of view, several papers have considered solving the c-LASSO problem using first-order algorithms [4], [21].<sup>5</sup> The deterministic framework that measures the convergence of an algorithm on the problem instance that yields the slowest convergence rate is not an appropriate measure of the convergence rate for the CS problems [15]. Therefore, Maleki and Baraniuk [15] consider the average convergence rate for iterative algorithms. In that setting, AMP is the only first-order al-

<sup>5</sup>First-order methods are iterative algorithms that use either the gradient or the subgradient of the function at the previous iterations to update their estimates.

gorithm that provably achieves linear convergence to date. Similarly, the CAMP algorithm, introduced in this paper, provides the first, first-order c-LASSO solver that provides a linear average convergence rate.

### G. Organization of this Paper

We introduce the CAMP algorithm in Section II. We then explain the SE equations that characterize the evolution of the MSE through the iterations of the CAMP algorithm in Section III, and we analyze the important properties of the SE equations. We then discuss the connection between our calculations and the solution of LASSO in Section III-D. We confirm our results via Monte Carlo simulations in Section IV.

## II. COMPLEX APPROXIMATE MESSAGE PASSING

The high computational complexity of interior point methods for solving large-scale convex optimization problems has spurred the development of first-order methods for solving the LASSO problem. See [15] and the references therein for a description of some of these algorithms. One of the most successful algorithms for CS problems is the AMP algorithm introduced in [3]. In this section, we use the approach introduced in [48] to derive the approximate message passing algorithm for the c-LASSO problem that we term CAMP.

Let  $s_1, s_2, \dots, s_N$  be  $N$  random variables with the following distribution:

$$p(s_1, s_2, \dots, s_N) = \frac{1}{Z(\beta)} e^{-\beta \lambda \|s\|_1 - \frac{\beta}{2} \|y - As\|_2^2} \quad (3)$$

where  $\beta$  is a constant and  $Z(\beta) \triangleq \int_s e^{-\beta \lambda \|s\|_1 - \frac{\beta}{2} \|y - As\|_2^2} ds$ . As  $\beta \rightarrow \infty$ , the mass of this distribution concentrates around the solution of the LASSO. Therefore, one way to find the solution of LASSO is to marginalize this distribution. However, calculating the marginal distribution is an NP-complete problem. The sum-product message passing algorithm provides a successful heuristic for approximating the marginal distribution. As  $N \rightarrow \infty$  and  $\beta \rightarrow \infty$ , the iterations of the sum-product message passing algorithm are simplified to (see [48] or [47, Ch. 5])

$$\begin{aligned} x_{\ell \rightarrow a}^{t+1} &= \eta \left( \sum_{b \neq a} A_{b\ell}^* z_{b \rightarrow \ell}^t; \tau_t \right) \\ z_{a \rightarrow \ell}^t &= y_a - \sum_{j \neq \ell} A_{aj} x_{j \rightarrow a}^t \end{aligned} \quad (4)$$

where  $\eta(u + iv; \lambda) \triangleq \left( u + iv - \frac{\lambda(u+iv)}{\sqrt{u^2+v^2}} \right)_+ \mathbb{1}_{\{u^2+v^2>\lambda^2\}}$  is the proximity operator of the complex  $\ell_1$ -norm and is called complex soft thresholding. See Section V-A for further information regarding this function.  $\tau_t$  is the threshold parameter at time  $t$ . The choice of this parameter will be discussed in Section III-A. The per-iteration computational complexity of this algorithm is high, since  $2nN$  messages  $x_{\ell \rightarrow a}^t$  and  $z_{a \rightarrow \ell}^t$  are updated. Therefore, following [48], we assume that there exist  $\Delta x_{\ell \rightarrow a}^t, \Delta z_{a \rightarrow \ell}^t = O(1/\sqrt{N})$  such that

$$\begin{aligned} x_{\ell \rightarrow a}^t &= x_{\ell}^t + \Delta x_{\ell \rightarrow a}^t + O(1/N) \\ z_{a \rightarrow \ell}^t &= z_a^t + \Delta z_{a \rightarrow \ell}^t + O(1/N). \end{aligned} \quad (5)$$

Here, the  $O(\cdot)$  errors are uniform in the choice of the edges  $\ell \rightarrow a$  and  $a \rightarrow \ell$ . In other words, we assume that  $x_{\ell \rightarrow a}^t$  is independent of  $a$  and  $z_{a \rightarrow \ell}^t$  is independent of  $\ell$  except for an error of order  $1/\sqrt{N}$ . For further discussion of this assumption and its validation, see [48] or [47, Ch. 5]. Let  $\eta^I$  and  $\eta^R$  be the imaginary and real parts of the complex soft thresholding function, respectively. Furthermore, define  $\frac{\partial \eta^R}{\partial x}$  and  $\frac{\partial \eta^R}{\partial y}$  as the partial derivatives of  $\eta^R$  with respect to the real and imaginary parts of the input, respectively.  $\frac{\partial \eta^I}{\partial x}$ , and  $\frac{\partial \eta^I}{\partial y}$  are defined similarly. The following theorem shows how one can simplify the message passing as  $N \rightarrow \infty$ .

*Proposition II.1:* Suppose that (5) holds for every iteration of the message passing algorithm specified in (4). Then,  $x_\ell^t$  and  $z_a^t$  satisfy the following equations:

$$\begin{aligned} x_\ell^{t+1} &= \eta \left( x_\ell^t + \sum_b A_{b\ell}^* z_b^t; \tau_t \right), \\ z_a^{t+1} &= y_a - \sum_j A_{aj} x_j^{t+1} \\ &\quad - \sum_j A_{aj} \left( \frac{\partial \eta^R}{\partial x} \left( x_j^t + \sum_b A_{bj}^* z_b^t \right) \right) \mathcal{R}(A_{aj}^* z_a^t) \\ &\quad - \sum_j A_{aj} \left( \frac{\partial \eta^R}{\partial y} \left( x_j^t + \sum_b A_{bj}^* z_b^t \right) \right) \mathcal{I}(A_{aj}^* z_a^t) \\ &\quad - i \sum_j A_{aj} \left( \frac{\partial \eta^I}{\partial x} \left( x_j^t + \sum_b A_{bj}^* z_b^t \right) \right) \mathcal{R}(A_{aj}^* z_a^t) \\ &\quad - i \sum_j A_{aj} \left( \frac{\partial \eta^I}{\partial y} \left( x_j^t + \sum_b A_{bj}^* z_b^t \right) \right) \mathcal{I}(A_{aj}^* z_a^t). \end{aligned} \quad (6)$$

See Section V-B for the proof. According to Proposition II.1 and (5), for large values of  $N$ , the messages  $x_{\ell \rightarrow a}^t$  and  $z_{a \rightarrow \ell}^t$  are close to  $x_\ell^t$  and  $z_a^t$  in (6). Therefore, we define the CAMP algorithm as the iterative method that starts from  $x^0 = 0$  and  $z^0 = y$  and uses the iterations specified in (6). It is important to note that Proposition II.1 does not provide any information on either the performance of the CAMP algorithm or the connection between CAMP and c-LASSO, since message passing is a heuristic algorithm and does not necessarily converge to the correct marginal distribution of (3).

### III. FORMAL ANALYSIS OF CAMP AND C-LASSO

In this section, we explain the SE framework that predicts the performance of the CAMP and c-LASSO in the asymptotic settings. We then use this framework to analyze the phase transition and noise sensitivity of the CAMP and c-LASSO. The formal connection between SE and CAMP/c-LASSO is discussed in Section III-D.

#### A. State Evolution

We now conduct an asymptotic analysis of the CAMP algorithm. As we confirm in Section III-D, the asymptotic performance of the algorithm is tracked through a few variables, called the state variables. The state of the algorithm is the five-tuple  $s = (m; \delta, \rho, \sigma, G)$ , where  $G$  corresponds to the distribution of the nonzero elements of the sparse vector  $s_o$ ,  $\sigma$  is the standard

deviation of the measurement noise, and  $m$  is the asymptotic normalized MSE. The threshold parameter (threshold policy) of CAMP in its most general form could be a function of the state of the algorithm  $\tau(s)$ . Define  $\text{npi}(m; \sigma, \delta) \triangleq \sigma^2 + \frac{m}{\delta}$ . The *MSE map* is defined as

$$\Psi(s, \tau(s)) \triangleq \mathbb{E} |\eta(X + \sqrt{\text{npi}(m, \sigma, \delta)} Z_1 + i \sqrt{\text{npi}(m, \sigma, \delta)} Z_2; \tau(s)) - X|^2$$

where  $Z_1, Z_2 \sim N(0, 1/2)$  and  $X \sim (1 - \rho\delta)\delta_0(|x|) + \rho\delta G(x)$  are independent random variables. Note that  $G$  is a probability distribution on  $\mathbb{C}$ . In the rest of this paper, we consider the thresholding policy  $\tau(s) = \tau \sqrt{\text{npi}(m, \sigma, \delta)}$ , where the constant  $\tau$  is yet to be tuned according to the schemes introduced in Sections I-D1 and I-D2. When we use this thresholding policy, we may equivalently write  $\Psi(s, \tau(s))$  as  $\Psi(s, \tau)$ . This thresholding policy is the same as the thresholding policy introduced in [3] and [11]. When the parameters  $\delta, \rho, \sigma, \tau$ , and  $G$  are clear from the context, we denote the MSE map by  $\Psi(m)$ . SE is the evolution of  $m$  (starting from  $t = 0$  and  $m_0 = E(|X|^2)$ ) by the rule

$$\begin{aligned} m_{t+1} &= \Psi(m_t) \\ &\triangleq \mathbb{E} \left| \eta \left( X + \sqrt{\text{npi}^t} Z_1 + i \sqrt{\text{npi}^t} Z_2; \tau \sqrt{\text{npi}^t} \right) - X \right|^2 \end{aligned} \quad (7)$$

where  $\text{npi}^t \triangleq \text{npi}(m_t, \sigma, \delta)$ . As will be described in Section III-D, this equation tracks the normalized MSE of the CAMP algorithm in the asymptotic setting  $n, N \rightarrow \infty$  and  $n/N \rightarrow \delta$ . In other words, if  $m_t$  is the MSE of the CAMP algorithm at iteration  $t$ , the  $m_{t+1}$ , calculated by (7), is the MSE of CAMP at iteration  $t + 1$ .

*Definition III.1:* Let  $\Psi$  be almost everywhere differentiable.  $m^*$  is called a fixed point of  $\Psi$  if and only if  $\Psi(m^*) = m^*$ . Furthermore, a fixed point is called stable if  $\left. \frac{d\Psi(m)}{dm} \right|_{m=m^*} < 1$ , and unstable if  $\left. \frac{d\Psi(m)}{dm} \right|_{m=m^*} > 1$ .

It is clear that if  $m^*$  is the unique stable fixed point of the  $\Psi$  function, then  $m_t \rightarrow m^*$  as  $t \rightarrow \infty$ . Also, if all the fixed points of  $\Psi$  are unstable, then  $m_t \rightarrow \infty$  as  $t \rightarrow \infty$ . Define  $\mu \triangleq |X|$  and  $\theta \triangleq \angle X$ . Let  $G(\mu, \theta)$  denote the probability density function of  $X$  and define  $G(\mu) \triangleq \int G(\mu, \theta) d\theta$  as the marginal distribution of  $\mu$ . The next lemma shows that in order to analyze the SE function, we only need to consider the amplitude distribution. This substantially simplifies our analysis of SE in the next sections.

*Lemma III.2:* The MSE map does not depend on the phase distribution of the input signal, i.e.,

$$\Psi(m, \delta, \rho, \sigma, G(\mu, \theta), \tau) = \Psi(m, \delta, \rho, \sigma, G(\mu), \tau).$$

See Section V-C for the proof.

#### B. Noise-Free Signal Recovery

Consider the noise free setting with  $\sigma = 0$ . Suppose that SE predicts the MSE of CAMP in the asymptotic setting (we will make this rigorous in Section III-D). As mentioned

in Section I-D1, in order to characterize the performance of CAMP in the noiseless setting, we first derive its phase transition curve and then optimize over  $\tau$  to obtain the highest phase transition CAMP can achieve. Fix all the state variables except for  $m$  and  $\rho$ . The evolution of  $m$  discriminates the following two regions for  $\rho$ :

Region I: The values of  $\rho$  for which  $\Psi(m) < m$  for every  $m > 0$ .

Region II: The complement of Region I.

Since 0 is necessarily a fixed point of the  $\Psi$  function, in Region I,  $m_t \rightarrow 0$  as  $t \rightarrow \infty$ . The following lemma shows that in Region II,  $m = 0$  is an unstable fixed point and therefore starting from  $m_0 \neq 0$ ,  $m_t \rightarrow 0$ .

*Lemma III.3:* Let  $\sigma = 0$ . If  $\rho$  is in Region II, then  $\Psi$  has an unstable fixed point at zero.

*Proof:* We prove in Lemma V.2 that  $\Psi(m)$  is a concave function of  $m$ . Therefore,  $\rho$  is in Region II if and only if  $\frac{d\Psi(m)}{dm} \Big|_{m=0} > 1$ . This, in turn, indicates that 0 is an unstable fixed point.

It is also easy to confirm that Region I is of the form  $[0, \rho_{SE}(\delta, G, \tau))$ . As we will see in Section III-D,  $\rho_{SE}(\delta, G, \tau)$  determines the phase transition curve of the CAMP algorithm. According to Lemma III.2, the MSE map does not depend on the phase distribution of the nonzero elements. The following proposition shows that in fact  $\rho_{SE}$  is independent of  $G$  even though the  $\Psi$  function depends on  $G(\mu)$ .

*Proposition III.4:*  $\rho_{SE}(\delta, G, \tau)$  is independent of the distribution  $G$ .

*Proof:* According to Lemma V.2 in Section V-D,  $\Psi$  is concave. Therefore, it has a stable fixed point at zero if and only if its derivative at zero is less than 1. It is also straightforward (from Section V-D) to show that

$$\frac{d\Psi}{dm} \Big|_{m=0} = \frac{\rho\delta(1+\tau^2)}{\delta} + \frac{1-\rho\delta}{\delta} \mathbb{E}|\eta(Z_1 + iZ_2; \tau)|^2.$$

Setting this derivative to 1, it is clear that the phase transition value of  $\rho$  is independent of  $G$ . ■

According to Proposition III.4, the only parameters that affect  $\rho_{SE}$  are  $\delta$  and the free parameter  $\tau$ . Fixing  $\delta$ , we tune  $\tau$  such that the algorithm achieves its highest phase transition for a certain number of measurements, i.e.,

$$\rho_{SE}(\delta) \triangleq \sup_{\tau} \rho_{SE}(\delta; \tau).$$

Using SE, we can calculate the optimal value of  $\tau$  and  $\rho_{SE}(\delta)$ .

*Theorem III.5:*  $\rho_{SE}(\delta)$  and  $\delta$  satisfy the following implicit relations:

$$\begin{aligned} \rho_{SE}(\delta) &= \frac{\chi_1(\tau)}{(1+\tau^2)\chi_1(\tau) - \tau\chi_2(\tau)} \\ \delta &= \frac{4(1+\tau^2)\chi_1(\tau) - 4\tau\chi_2(\tau)}{-2\tau + 4\chi_2(\tau)} \end{aligned}$$

for  $\tau \in [0, \infty)$ . Here,  $\chi_1(\tau) \triangleq \int_{\omega \geq \tau} \omega(\tau - \omega)e^{-\omega^2} d\omega$  and  $\chi_2(\tau) \triangleq \int_{\omega > \tau} \omega(\omega - \tau)^2 e^{-\omega^2}$ .

See Section V-D for the proof. Fig. 1 displays this phase transition curve that is derived from the SE framework and compares it with the phase transition of r-BP algorithm. As will

be described later,  $\rho_{SE}(\delta)$  corresponds to the phase transition of c-LASSO. Hence, the difference between  $\rho_{SE}(\delta)$  and phase transition curve of r-LASSO is the benefit of grouping the real and imaginary parts.

It is also interesting to compare the  $\rho_{SE}(\delta)$  (which as we see later predicts the performance of c-LASSO) with the phase transition of r-LASSO in high undersampling regime  $\delta \rightarrow 0$ . The implicit formulation above enables us to calculate the asymptotic performance of the phase transition as  $\delta \rightarrow 0$ .

*Theorem III.6:*  $\rho_{SE}(\delta)$  follows the asymptotic behavior

$$\rho_{SE}(\delta) \sim \frac{1}{\log(\frac{1}{2\delta})}, \text{ as } \delta \rightarrow 0.$$

See Section V-E for the proof. As mentioned above, this theorem shows that as  $\delta \rightarrow 0$ , the phase transition of c-BP and CAMP is two times that of the r-LASSO, which is given by  $\rho_{SE}^R \sim 1/(2\log(1/\delta))$ [19]. This improvement is due to the grouping of real and imaginary parts of the signal.

### C. Noise Sensitivity

In this section, we characterize the noise sensitivity of SE. To achieve this goal, we first discuss the risk of the complex soft thresholding function. The properties of this risk play an important role in the discussion of the noise sensitivity of SE in Section III-C2.

*1) Risk of Soft Thresholding:* Define the risk of the soft thresholding function as

$$r(\mu, \tau) \triangleq \mathbb{E}|\eta(\mu e^{i\theta} + Z_1 + iZ_2; \tau) - X|^2$$

where  $\mu \in [0, \infty)$ ,  $\theta \in [0, 2\pi]$ , and the expected value is with respect to the two independent random variables  $Z_1, Z_2 \sim N(0, 1/2)$ . It is important to note that according to Lemma III.2, the risk function is independent of  $\theta$ . The following lemma characterizes two important properties of this risk function.

*Lemma III.7:*  $r(\mu, \tau)$  is an increasing function of  $\mu$  and a concave function in terms of  $\mu^2$ .

See Section V-F for the proof of this lemma. We define the minimax risk of the soft thresholding function as

$$M^b(\epsilon) \triangleq \inf_{\tau > 0} \sup_{q \in \mathcal{F}_\epsilon} \mathbb{E}|\eta(X + Z_1 + iZ_2; \tau) - X|^2$$

where  $q$  is the probability density function of  $X$ , and the expected value is with respect to  $X, Z_1$  and  $Z_2$ .

Note that  $q \in \mathcal{F}_\epsilon$  implies that  $q$  has a point mass of  $1 - \epsilon$  at zero; see Section I-C for more information. In the next section, we show a connection between this minimax risk and the noise sensitivity of the SE. Therefore, it is important to characterize  $M^b(\epsilon)$ .

*Proposition III.8:* The minimax risk of the soft thresholding function satisfies

$$M^b(\epsilon) = \inf_{\tau} 2(1 - \epsilon) \int_{w=\tau}^{\infty} w(w - \tau)^2 e^{-w^2} dw + \epsilon(1 + \tau^2). \quad (8)$$

See Section V-G for the proof. It is important to note that the quantities in (8) can be easily calculated in terms of the density and distribution function of a normal random variable. Therefore, a simple computer program may accurately calculate the value of  $M^b(\epsilon)$  for any  $\epsilon$ .

The proof provided for Proposition III.8 also proves the following proposition. We will discuss the importance of this result for CS problems in the next section.

*Proposition III.9:* The maximum of the risk function,  $\max_{q \in \mathcal{F}_{\epsilon,\gamma}} \mathbb{E}|\eta(X + Z_1 + iZ_2; \tau) - X|^2$ , is achieved on  $q(X) = (1 - \epsilon)\delta_0(|X|) + \epsilon\delta_\gamma(|X|)$ .

First, note that the maximizing distribution (or least favorable distribution) is independent of the threshold parameter. Second, note that the maximizing distribution is not unique since we have already proved that the phase distribution does not affect the risk function.

2) *Noise Sensitivity of SE:* As mentioned in Section III-A, in the presence of measurement noise, SE is given by

$$\begin{aligned} m_{t+1} &= \Psi(m_t) \\ &= \mathbb{E}|\eta(X + \sqrt{\text{npi}}Z_1 + i\sqrt{\text{npi}}Z_2; \tau\sqrt{\text{npi}}) - X|^2 \end{aligned}$$

where  $\text{npi} = \sigma^2 + \frac{m_t}{\delta}$ . As mentioned above,  $m_t$  characterizes the asymptotic MSE of CAMP at iteration  $t$ . Therefore, the final solution of the CAMP algorithm converges to one of the stable fixed points of the  $\Psi$  function. The next theorem suggests that the stable fixed point is unique, and therefore, no matter where the algorithm starts from it will always converge to the same MSE.

*Lemma III.10:*  $\Psi(m)$  has a unique stable fixed point to which the sequence of  $\{m_t\}$  converges.

We call the fixed point in Lemma III.10  $\text{fMSE}(\sigma^2, \delta, \rho, G, \tau)$ . According to Section I-D2, we define the minimax noise sensitivity as

$$\text{NS}^{\text{SE}}(\delta, \rho) \triangleq \min_{\tau} \sup_{\sigma > 0} \sup_{q \in \mathcal{F}_\epsilon} \text{fMSE}(\sigma^2, \delta, \rho, G, \tau) / \sigma^2.$$

The noise sensitivity of SE can be easily evaluated from  $M^\flat(\epsilon)$ . The following theorem characterizes this relation.

*Theorem III.11:* Let  $\rho_{\text{MSE}}(\delta)$  be the value of  $\rho$  satisfying  $M^\flat(\rho\delta) = \delta$ . Then, for  $\rho < \rho_{\text{MSE}}$ , we have

$$\text{NS}^{\text{SE}}(\delta, \rho) = \frac{M^\flat(\delta\rho)}{1 - M^\flat(\delta\rho)/\delta}$$

and for  $\rho > \rho_{\text{MSE}}(\delta)$ ,  $\text{NS}^{\text{SE}}(\delta, \rho) = \infty$ .

The proof of this theorem follows along the same lines as the proof of Proposition 3.1 in [11], and therefore, we skip it for the sake of brevity. The contour lines of this noise sensitivity function are displayed in Fig. 2.

Similar arguments as those presented in Proposition 3.1 in [11] combined with Proposition III.9 prove the following.

*Proposition III.12:* The maximum of the formal MSE,  $\max_{q \in \mathcal{F}_{\epsilon,\gamma}} \text{fMSE}(\sigma^2, \delta, \rho, G, \tau)$  is achieved by  $q = (1 - \epsilon)\delta_0(|X|) + \epsilon\delta_\gamma(|X|)$ , independent of  $\sigma$  and  $\tau$ .

Again we emphasize that the maximizing or least favorable distribution is not unique. Note that the least favorable distribution provides a simple approach for designing and setting the parameters of CS systems [8]: We design the system such that it performs well on the least favorable distribution, and it is then guaranteed that the system will perform as well (or in many cases better) on all other input distributions.

As a final remark, we note that  $\rho_{\text{MSE}}(\delta)$  equals  $\rho_{\text{SE}}(\delta)$  as proved next.

*Proposition III.13:* For every  $\delta \in [0, 1]$ , we have

$$\rho_{\text{MSE}}(\delta) = \rho_{\text{SE}}(\delta).$$

*Proof:* The proof is a simple comparison of the formulas. We first know that  $\rho_{\text{MSE}}$  is derived from the following equation:

$$\min_{\tau} 2(1 - \rho\delta) \int_{\omega > \tau} \omega(\omega - \tau)^2 e^{-\omega^2} d\omega + \rho\delta(1 + \tau^2) = \delta.$$

On the other hand, since  $\Psi(m)$  is a concave function of  $m$ ,  $\rho_{\text{SE}}(\delta, \tau)$  is derived from  $\frac{d\Psi(m)}{dm} \Big|_{m=0} = 1$ . This derivative is equal to

$$\frac{d\Psi(m)}{dm} \Big|_{m=0} = \frac{2(1 - \rho\delta)}{\delta} \int_{\omega > \tau} \omega(\omega - \tau)^2 e^{-\omega^2} d\omega + \frac{\rho\delta}{\delta}(1 + \tau^2).$$

Also,  $\rho_{\text{SE}}(\delta) = \sup_{\tau} \rho_{\text{SE}}(\tau, \delta)$ . However, in order to obtain the highest  $\rho$ , we should minimize the above expression over  $\tau$ . Therefore, both  $\rho_{\text{SE}}(\delta)$  and  $\rho_{\text{MSE}}(\delta)$  satisfy the same equations and thus are exactly equal. ■

#### D. Connection Between the SE, CAMP, and C-LASSO

There is a strong connection between the SE framework, the CAMP algorithm, and c-LASSO. Recently, Bayati and Montanari [16] proved that SE predicts the asymptotic performance of the AMP algorithm when the measurement matrix is i.i.d. Gaussian. The result also holds for complex Gaussian matrices and complex input vectors. As in [3], we conjecture that the SE predictions are correct for a “large” class of random matrices. We show evidence of this claim in Section IV. Here, for the sake of completeness, we quote the result of [16] in the complex setting. Let  $\gamma : \mathbb{C}^2 \rightarrow \mathbb{R}$  be a pseudo-Lipschitz function.<sup>6</sup> To make the presentation clear, we consider a simplified version of Definition 1 in [46].

*Definition III.14:* A sequence of instances  $\{s_o(N), A(N), w(N)\}$ , indexed by the ambient dimension  $N$ , is called a converging sequence if the following conditions hold.

- 1) The elements of  $s_o(N) \in \mathbb{R}^N$  are i.i.d. drawn from  $(1 - \rho\delta)\delta_0(|s_{o,i}|) + \rho\delta G(s_{o,i})$ .
- 2) The elements of  $w(N) \in \mathbb{R}^n$  ( $n = \delta N$ ) are i.i.d. drawn from  $N(0, \sigma_w^2)$ .
- 3) The elements of  $A(N) \in \mathbb{R}^{n \times N}$  are i.i.d. drawn from a complex Gaussian distribution.

*Theorem III.15:* Consider a converging sequence  $\{s_o(N), A(N), w(N)\}$ . Let  $x^t(N)$  be the estimate of the CAMP algorithm at iteration  $t$ . For any pseudo-Lipschitz function  $\gamma : \mathbb{C}^2 \rightarrow \mathbb{R}$ , we have

$$\begin{aligned} \lim_{N \rightarrow \infty} \frac{1}{N} \sum_{i=1}^N \gamma(x_i^t, s_{o,i}) \\ = \mathbb{E}\gamma\left(\eta\left(X + \sqrt{\text{npi}^t}Z_1 + i\sqrt{\text{npi}^t}Z_2; \tau\sqrt{\text{npi}^t}\right), X\right) \end{aligned}$$

almost surely, where  $Z_1 + iZ_2 \sim CN(0, 1)$  and  $X \sim (1 - \rho\delta)\delta_0(|s_{o,i}|) + \rho\delta G(s_{o,i})$  are independent complex random variables. Also,  $\text{npi}^t \triangleq \sigma^2 + m_t/\delta$ , where  $m_t$  satisfies (7).

<sup>6</sup> $\gamma : \mathbb{C}^2 \rightarrow \mathbb{R}$  is pseudo-Lipschitz if and only if  $|\psi(x) - \psi(y)| \leq L(1 + \|x\|_2 + \|y\|_2)\|x - y\|_2$ .

The proof of this theorem is similar to the proof of Theorem 1 in [16] and hence is skipped here.

It is also straightforward to extend the result of [11] and [46] on the connection of message passing algorithms and LASSO to the complex setting. For a given value of  $\tau$ , suppose that the fixed point of the SE is denoted by  $m^*$ . Define  $\lambda(\tau)$  as

$$\lambda(\tau) \triangleq \tau \sqrt{m^*} \left( 1 - \frac{1}{2\delta} \mathbb{E} \left( \frac{\partial \eta^R}{\partial x} + \frac{\partial \eta^I}{\partial y} \right) \right) \quad (9)$$

where

$$\begin{aligned} \frac{\partial \eta^R}{\partial x} &\triangleq \frac{\partial \eta^R}{\partial x} \left( X + \sqrt{m^*} Z_1 + i \sqrt{m^*} Z_2; \tau \sqrt{m^*} \right) \\ \frac{\partial \eta^I}{\partial y} &\triangleq \frac{\partial \eta^I}{\partial y} \left( X + \sqrt{m^*} Z_1 + i \sqrt{m^*} Z_2; \tau \sqrt{m^*} \right) \end{aligned}$$

and  $\mathbb{E}$  is with respect to independent random variables  $Z_1 + iZ_2 \sim CN(0, 1)$  and  $X \sim (1 - \rho\delta)\delta_0(|s_{o,i}|) + \rho\delta G(s_{o,i})$ . The following theorem establishes the connection between the solution of LASSO and the SE equation.

**Theorem III.16:** Consider a converging sequence  $\{s_o(N), A(N), w(N)\}$ . Let  $\hat{x}^{\lambda(\tau)}(N)$  be the solution of LASSO. Then, for any pseudo-Lipschitz function  $\gamma : \mathbb{C}^2 \rightarrow \mathbb{R}$ , we have

$$\begin{aligned} \lim_{N \rightarrow \infty} \frac{1}{N} \sum_{i=1}^N \gamma(\hat{x}_i^{\lambda(\tau)}(N), s_{o,i}) \\ = \mathbb{E} \gamma \left( \eta \left( X + \sqrt{n\pi^*} Z_1 + i \sqrt{n\pi^*} Z_2; \tau \sqrt{n\pi^*} \right), X \right) \end{aligned}$$

almost surely, where  $Z_1 + iZ_2 \sim CN(0, 1)$  and  $X \sim (1 - \rho\delta)\delta_0(|s_{o,i}|) + \rho\delta G(s_{o,i})$  are independent complex random variables.  $n\pi^* \triangleq \sigma^2 + m^*/\delta$ , where  $m^*$  is the fixed point of (7).

The proof of the theorem is similar to the proof of Theorem 1.4 in [46] and hence is skipped here.

Note that according to Theorems III.15 and III.16, SE predicts the dynamic of the AMP algorithm and the solution of LASSO accurately in the asymptotic settings.

## E. Discussion

1) *Convergence Rate of CAMP:* In this section, we briefly discuss the convergence rate of the CAMP algorithm. In this respect, our results are straightforward extension of the analysis in [15]. But, for the sake of completeness, we mention a few highlights. Let  $\{m_t\}_{t=1}^\infty$  be a sequence of MSE generated according to SE (7) for  $X \sim (1 - \epsilon)\delta_0(|X|) + \epsilon G(X), \tau$ , and  $\sigma^2 = 0$ . The following proposition provides an upper bound on  $m_t$  as a function of iteration  $t$ .

**Theorem III.17:** Let  $\{m_t\}_{t=1}^\infty$  be a sequence of MSEs generated according to SE. Then

$$m^t \leq \left( \frac{d\Psi(m)}{dm} \Big|_{m=0} \right)^t m_0.$$

*Proof:* Since according to Lemma V.2  $\Psi(m)$  is concave, we have  $\Psi(m) \leq \frac{d\Psi(m)}{dm} \Big|_{m=0} m$ . Hence, at every iteration,  $m$  is attenuated by  $\frac{d\Psi(m)}{dm} \Big|_{m=0}$ . After  $t$  iterations, we have  $m^t \leq \left( \frac{d\Psi(m)}{dm} \Big|_{m=0} \right)^t m_0$ .

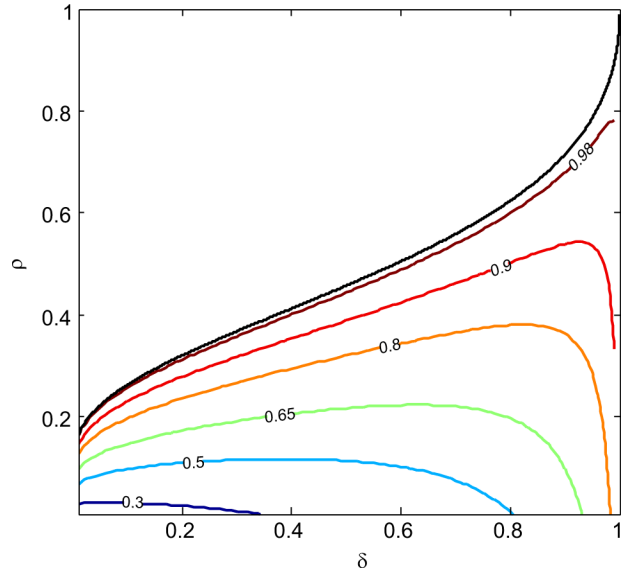


Fig. 4. Contour lines of  $\frac{d\Psi(m)}{dm} \Big|_{m=0}$  as a function of  $\rho$  and  $\delta$ . The parameter  $\tau$  in the SE is set according to Theorem III.5. The black curve is the phase transition of CAMP. The colored lines display the level sets of  $\frac{d\Psi(m)}{dm} \Big|_{m=0} = 0.3, 0.5, 0.65, 0.8, 0.9, 0.98$ . Note that according to Proposition III.17, if  $\frac{d\Psi(m)}{dm} \Big|_{m=0} < 0.9$ , then  $m_{200} < 7.1 \times 10^{-10} m_0$ .

According to Theorem III.17, the convergence rate of CAMP is linear (in the asymptotic setting).<sup>7</sup> In fact, due to the concavity of the  $\Psi$  function, CAMP converges faster for large values of MSE  $m$ . As  $m$  reaches zero, the convergence rate decreases toward the rate predicted by this theorem. Theorem III.17 provides an upper bound on the number of iterations the algorithm requires to reach to a certain accuracy. Fig. 4 exhibits the value of  $\frac{d\Psi(m)}{dm} \Big|_{m=0}$  as a function of  $\rho$  and  $\delta$ . This figure is based on the calculations we have presented in Section V-D. Here,  $\tau$  is chosen such that the CAMP algorithm achieves the same phase transition as c-BP algorithm. Note that, according to Proposition III.17, if  $\frac{d\Psi(m)}{dm} \Big|_{m=0} < 0.9$ , then  $m_{200} < 7.1 \times 10^{-10} m_0$ .

Theorem III.17 only considers the noise-free problem. But, again due to the concavity of the  $\Psi$  function, the convergence of CAMP to its fixed point is even faster for noisy measurements. To see this, note that once the measurements are noisy, the fixed point of CAMP occurs at a larger value of  $m$ . Since  $\Psi$  is concave, the derivative at this point is lower than the derivative at zero. Hence, convergence will be faster.

2) *Extensions:* The results presented in this paper are concerned with the two most popular problems in CS, i.e., exact recovery of sparse signals and approximate recovery of sparse signals in the presence of noise. However, our framework is far more powerful and can address other CS problems as well. For instance, a similar framework has been used to address the problem of recovering approximately sparse signals in the presence of noise [56]. For the sake of brevity, we have not provided such an analysis in this paper. However, the properties we proved in Lemmas III.2, III.7, and Proposition III.8 enable a straightforward extension of our analysis to such cases as well.

<sup>7</sup>If the measurement matrix is not i.i.d. random, CAMP does not necessarily converge at this rate. This is due to the fact that SE does not necessarily hold for arbitrary matrices.

Furthermore, the framework we developed here provides a way for recovering sparse complex-valued signals when the distribution of nonzero elements is known. This area has been studied in [12] and [51].

#### IV. SIMULATIONS

As explained in Section III-D, our theoretical results show that, if the elements of the matrix are i.i.d. Gaussian, then SE predicts the performance of the CAMP and c-LASSO algorithms accurately. However, in this section, we will show evidence that suggests the theoretical framework is applicable to a wider class of measurement matrices. We then investigate the dependence of the empirical phase transition on the input distribution for medium problem sizes.

##### A. Measurement Matrix Simulations

We investigate the effect of the measurement matrix distribution on the performance of CAMP and c-LASSO in two different cases. First, we consider the case where the measurements are noise-free. We postpone a discussion of measurement noise to Section IV-A2.

1) *Noise-Free Measurements*: Suppose that the measurements are noise-free. Our goal is to empirically measure the phase transition curves of the c-LASSO and CAMP on the measurement matrices provided in Table I. To characterize the phase transition of an algorithm, we do the following.

- 1) We consider 33 equispaced values of  $\delta$  between 0 and 1.
- 2) For each value of  $\delta$ , we calculate  $\rho_{\text{SE}}(\delta)$  from the theoretical framework and then consider 41 equispaced values of  $\rho$  in  $[\rho_{\text{SE}}(\delta) - 0.2, \rho_{\text{SE}}(\delta) + 0.2]$ .
- 3) We fix  $N = 1000$ , and for any value of  $\rho$  and  $\delta$ , we calculate  $n = \lfloor \delta N \rfloor$  and  $k = \lfloor \rho N \rfloor$ .
- 4) We draw  $M = 20$  independent random matrices from one of the distributions described in Table I, and for each matrix, we construct a random input vector  $s_o$  with one of the distributions described in Table II. We then form  $y = As_o$  and recover  $s_o$  from  $y$  and  $A$  by either c-BP or CAMP to obtain  $\hat{x}$ . The matrix distributions and coefficient distributions we consider in our simulations are specified in Tables I and II, respectively.
- 5) For each  $\delta$ ,  $\rho$ , and Monte Carlo sample  $j$ , we define a success variable  $S_{\delta,\rho,j} = \mathbb{I}\left(\frac{\|\hat{x}-x\|_2}{\|x\|_2} < \text{tol}\right)$  and we calculate the success probability  $\hat{p}_{\delta,\rho}^S = \frac{1}{M} \sum_j S_{\delta,\rho,j}$ . This provides an empirical estimate of the probability of correct recovery. The value of tol in our case is set to  $10^{-4}$ .
- 6) For a fixed value of  $\delta$ , we fit a logistic regression function to  $\hat{p}^S(\delta, \rho)$  to obtain  $p_{\delta}^S(\rho)$ . Then, we find the value of  $\hat{\rho}_{\delta}$  for which  $p_{\delta}^S(\rho) = 0.5$ .

See [6] for a more detailed discussion of this approach. For the c-LASSO algorithm, we are reproducing the experiments of [57] and [58], and, therefore, we are using one-L1 algorithm [57]. Although Fig. 4 confirms that for most cases even 200 iterations of CAMP are enough to reach convergence, since our goal is to measure the phase transition, we consider 3000 iterations. See Section III-E1 for the discussion on the convergence rate.

Fig. 5 compares the phase transition of c-LASSO and CAMP on the ensembles specified in Table I with the theoretical pre-

TABLE I  
ENSEMBLES CONSIDERED FOR THE MEASUREMENT MATRIX  $A$  IN THE MATRIX UNIVERSALITY ENSEMBLE EXPERIMENTS

Name	Specification
Gaussian	i.i.d. elements with $CN(0, 1/n)$
Rademacher	i.i.d. elements with real and imaginary parts distributed according to $\frac{1}{2}\delta - \sqrt{\frac{1}{2n}}(x) + \frac{1}{2}\delta\sqrt{\frac{1}{2n}}(x)$
Ternary	i.i.d. elements with real and imaginary parts distributed according to $\frac{1}{3}\delta - \sqrt{\frac{3}{2n}}(x) + \frac{1}{3}\delta_0(x) + \frac{1}{3}\delta\sqrt{\frac{3}{2n}}(x)$

TABLE II  
COEFFICIENT ENSEMBLES CONSIDERED IN COEFFICIENT ENSEMBLE EXPERIMENTS

Name	Specification
UP	i.i.d. elements with amplitude 1 and uniform phase
ZP	i.i.d. elements with amplitude 1 and phase zero
GA	i.i.d. elements with standard normal real and imaginary parts
UF	i.i.d. elements with $U[0, 1]$ real and imaginary parts

diction of this paper. In this simulation, the coefficient ensemble is UP (see Table II). Clearly, the empirical and theoretical phase transitions of the algorithms coincide. More importantly, we can conjecture that the choice of the measurement matrix ensemble does not affect the phase transition of these two algorithms. We will next discuss the impact of measurement matrix when there is noise on the measurements.

2) *Noisy Measurements*: In this section, we aim to show that, even in the presence of noise, the matrix ensembles defined in Table I perform similarly. Here is the setup for our experiment.

- 1) We set  $\delta = 0.25$ ,  $\rho = 0.1$ , and  $N = 1000$ .
- 2) We choose 50 different values of  $\sigma$  in the range  $[0.001, 0.1]$ .
- 3) We choose  $n \times N$  measurement matrix  $A$  from one of the ensembles specified in Table I.
- 4) We draw  $k$  i.i.d. elements from UP ensemble for the  $k = \lfloor \rho n \rfloor$  nonzero elements of the input  $s_o$ .
- 5) We form the measurement vector  $y = As_o + \sigma w$  where  $w$  is the noise vector with i.i.d. elements from  $CN(0, 1)$ .
- 6) For CAMP, we set  $\tau = 2$ . For c-LASSO, we use (9) to derive the corresponding values of  $\lambda$  for  $\tau = 2$  in CAMP.
- 7) We calculate the MSE  $\|\hat{x} - s_o\|_2^2/N$  for each matrix ensemble and compare the results.

Figs. 6 and 7 summarize our results. The concentration of the points along the  $y = x$  line indicates that the matrix ensembles, specified in Table I, perform similarly. The coincidence of the phase transition curves for different matrix ensembles is known as *universality hypothesis (conjecture)*. In order to provide a stronger evidence, we run the above experiment with  $N = 4000$ . The results of this experiment are exhibited in Figs. 8 and 9. It is clear from these figures that the MSE is now more concentrated around the  $y = x$  line. Additional experiments with other parameter values exhibited the same behavior. Note that as  $N$  grows, the variance of the MSE estimate becomes smaller, and the behavior of the algorithm is closer to the average performance that is predicted by the SE equation.

##### B. Coefficient Ensemble Simulations

According to Proposition III.4,  $\rho_{\text{SE}}(\delta, \tau)$  is independent of the distribution  $G$  of nonzero coefficients of  $s_o$ . We test the accuracy of this result on medium problem sizes. We fix  $\delta$  to

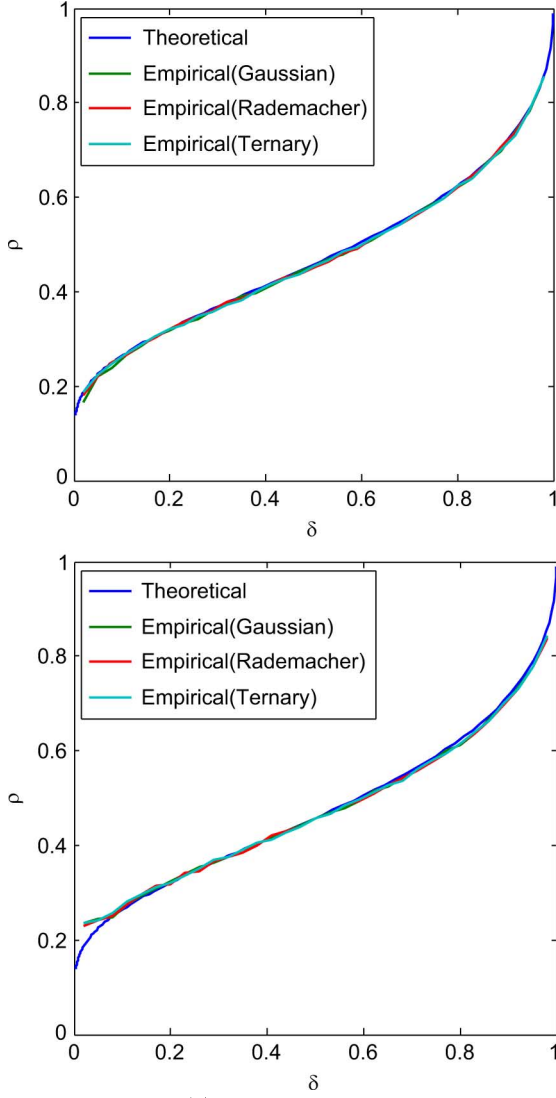


Fig. 5. Comparison of  $\rho_{\text{SE}}(\delta)$  with the empirical phase transition of c-LASSO [57] (top) and CAMP (bottom). There is a close match between the theoretical prediction and the empirical results from Monte Carlo simulations.

0.1 and we calculate  $\hat{p}_{\delta,\rho}^S$  for 60 equispaced values of  $\rho$  between 0.1 and 0.5. For each algorithm and each value of  $\rho$ , we run 100 Monte Carlo trials and calculate the success rate for the Gaussian matrix and the coefficient ensembles specified in Table II. Fig. 10 summarizes our result. Simulations at other values of  $\delta$  result in very similar behavior. These results are consistent with Proposition III.4. The small differences between the empirical phase transitions are due to two issues that are not reflected in Proposition III.4: 1)  $N$  is finite, while Proposition III.4 considers the asymptotic setting. 2) The number of algorithm iterations is finite, while Proposition III.4 assumes that we run CAMP for an infinite number of iterations.

## V. PROOFS OF THE MAIN RESULTS

### A. Proximity Operator

For a given convex function  $f : \mathbb{C}^n \rightarrow \mathbb{R}$ , the proximity operator at point  $x$  is defined as

$$\text{Prox}_f(x) \triangleq \arg \min_{y \in \mathbb{C}^n} \frac{1}{2} \|y - x\|_2^2 + f(y). \quad (10)$$

The proximity operator plays an important role in optimization theory. For further information, refer to [59] or [47, Ch. 7]. The

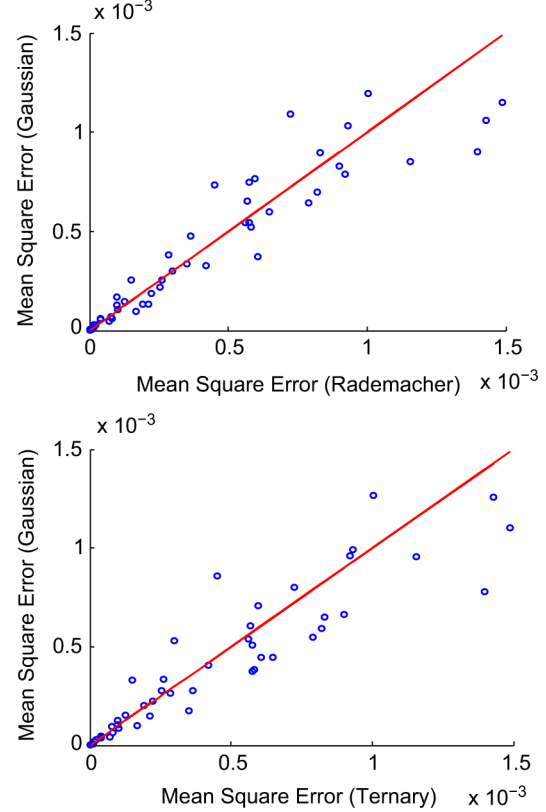


Fig. 6. Comparison of the MSE of c-LASSO for Gaussian and Rademacher matrix ensembles (top), and Gaussian and Ternary ensemble (bottom). The concentration of points around the  $y = x$  confirms the universality hypothesis. The norms of residuals are equal to  $5.9 \times 10^{-4}$  and  $6 \times 10^{-4}$  for the top and bottom figures, respectively. Comparison of this figure with Fig. 8 confirms that as  $N$  grows, the points become more concentrated around  $y = x$  line.

following lemma characterizes the proximity operator for the complex  $\ell_1$ -norm. This proximity operator has been used in several other papers [4], [21]–[23], [57].

*Lemma V.1:* Let  $f$  denote the complex  $\ell_1$ -norm function, i.e.,  $f(x) = \sum_i \sqrt{(x_i^R)^2 + (x_i^I)^2}$ . Then, the proximity operator is given by

$$\text{Prox}_{\tau f}(x) = \eta(x; \tau)$$

where  $\eta(u + iv; \tau) = \left( u + iv - \frac{\tau(u + iv)}{\sqrt{u^2 + v^2}} \right)_+$  is applied componentwise to the vector  $x$ .

*Proof:* Since (10) can be decoupled into the elements of the  $x, y$ , we can obtain the optimal value of  $y$ , by optimizing over its individual components. In other words, we solve the optimization in (10) for  $x, y \in \mathbb{C}$ . In this case, the optimization reduces to

$$\text{Prox}_{\tau f}(x) = \arg \min_{y \in \mathbb{C}} \frac{1}{2} |y - x|^2 + \tau |y|.$$

Suppose that the optimal  $y_*$  satisfies  $(y_*^R)^2 + (y_*^I)^2 > 0$ . Then, the function  $\sqrt{(y^R)^2 + (y^I)^2}$  is differentiable and the optimal solution satisfies

$$\begin{aligned} x^R - y_*^R &= \frac{\tau y_*^R}{\sqrt{(y_*^R)^2 + (y_*^I)^2}} \\ x^I - y_*^I &= \frac{\tau y_*^I}{\sqrt{(y_*^R)^2 + (y_*^I)^2}}. \end{aligned} \quad (11)$$

Combining the two equations in (11), we obtain  $y_*^R x^I = x^R y_*^I$ . Replacing this in (11), we have  $y_*^R = x^R - \frac{\tau |x^R|}{\sqrt{(x^R)^2 + (x^I)^2}}$  and

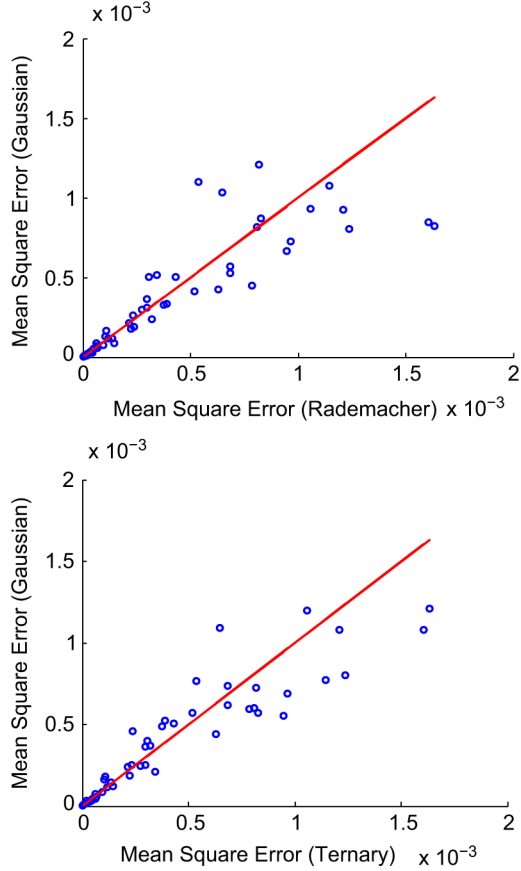


Fig. 7. Comparison of the MSE of CAMP for Gaussian and Rademacher matrix ensembles (top), and Gaussian and Ternary ensemble (bottom). The concentration of points around the  $y = x$  line confirms the universality hypothesis. The norms of residuals are equal to  $9.1 \times 10^{-4}$  and  $9.4 \times 10^{-4}$  for the top and bottom figures, respectively. Comparison of this figure with Fig. 9 confirms that as  $N$  grows, the points become more concentrated around  $y = x$  line.

$y_*^I = x^I - \frac{\tau |x^I|}{\sqrt{(x^R)^2 + (x^I)^2}}$ . It is clear that if  $\sqrt{(x^R)^2 + (x^I)^2} < \tau$ , then the signs of  $y_*^R$  and  $x^R$  will be opposite, which is in contradiction with (11). Therefore, if  $\sqrt{(x^R)^2 + (x^I)^2} < \tau$ , both  $y_*^R$  and  $y_*^I$  are zero. It is straightforward to check that  $(0, 0)$  satisfies the subgradient optimality condition. ■

### B. Proof of Proposition II.1

Let

$$\begin{aligned} \eta^R(x + iy) &\stackrel{\Delta}{=} \mathcal{R}(\eta(x + iy; \lambda)), \\ \eta^I(x + iy) &\stackrel{\Delta}{=} \mathcal{I}(\eta(x + iy; \lambda)) \end{aligned} \quad (12)$$

denote the real and imaginary parts of the complex soft thresholding function. Define

$$\begin{aligned} \partial_1 \eta^R &\stackrel{\Delta}{=} \frac{\partial \eta^R(x + iy)}{\partial x} \\ \partial_2 \eta^R &\stackrel{\Delta}{=} \frac{\partial \eta^R(x + iy)}{\partial y} \\ \partial_1 \eta^I &\stackrel{\Delta}{=} \frac{\partial \eta^I(x + iy)}{\partial x} \\ \partial_2 \eta^I &\stackrel{\Delta}{=} \frac{\partial \eta^I(x + iy)}{\partial y}. \end{aligned} \quad (13)$$

We first simplify the expression for  $z_{a \rightarrow \ell}^t$ :

$$\begin{aligned} z_{a \rightarrow \ell}^t &= y_a - \underbrace{\sum_{j \in [N]} A_{aj} x_j^t}_{z_a^t \stackrel{\Delta}{=}} - \underbrace{\sum_{j \in [N]} A_{aj} \Delta x_{j \rightarrow a}^t}_{\Delta z_{a \rightarrow \ell}^t \stackrel{\Delta}{=}} \\ &+ \underbrace{A_{a\ell} x_\ell^t}_{\Delta z_{a \rightarrow \ell}^t} + O(1/N). \end{aligned} \quad (14)$$

We also use the first-order expansion of the soft thresholding function to obtain

$$\begin{aligned} x_{\ell \rightarrow a}^{t+1} &= \eta \left( \sum_{b \in [n]} A_{b\ell}^* z_b^t + \sum_{b \in [n]} A_{b\ell}^* \Delta z_{b \rightarrow \ell}^t - A_{a\ell}^* z_a^t; \tau_t \right) \\ &+ O\left(\frac{1}{N}\right) \\ &= \eta \left( \sum_{b \in [n]} A_{b\ell}^* z_b^t + \sum_{b \in [n]} A_{b\ell}^* \Delta z_{b \rightarrow \ell}^t; \tau_t \right) \\ &\quad \underbrace{\qquad \qquad \qquad}_{x_\ell^t \stackrel{\Delta}{=}} \\ &- \mathcal{R}(A_{a\ell}^* z_a^t) \partial_1 \eta^R \left( \sum_{b \in [n]} A_{b\ell}^* z_b^t + \sum_{b \in [n]} A_{b\ell}^* \Delta z_{b \rightarrow \ell}^t \right) \\ &- \mathcal{I}(A_{a\ell}^* z_a^t) \partial_2 \eta^R \left( \sum_{b \in [n]} A_{b\ell}^* z_b^t + \sum_{b \in [n]} A_{b\ell}^* \Delta z_{b \rightarrow \ell}^t \right) \\ &- \mathcal{R}(A_{a\ell}^* z_a^t) \partial_1 \eta^I \left( \sum_{b \in [n]} A_{b\ell}^* z_b^t + \sum_{b \in [n]} A_{b\ell}^* \Delta z_{b \rightarrow \ell}^t \right) \\ &- \mathcal{I}(A_{a\ell}^* z_a^t) \partial_2 \eta^I \left( \sum_{b \in [n]} A_{b\ell}^* z_b^t + \sum_{b \in [n]} A_{b\ell}^* \Delta z_{b \rightarrow \ell}^t \right) \\ &+ O\left(\frac{1}{N}\right). \end{aligned} \quad (15)$$

According to (14),  $\Delta z_{b \rightarrow \ell}^t = A_{b\ell} x_\ell^t$ . Furthermore, we assume that the columns of the matrix are normalized. Therefore,  $\sum_b A_{b\ell}^* \delta z_{b \rightarrow \ell}^t = x_\ell^t$ . It is also clear that

$$\begin{aligned} \Delta x_{\ell \rightarrow a}^t &\stackrel{\Delta}{=} -\mathcal{R}(A_{a\ell}^* z_a^t) \partial_1 \eta^R \left( \sum_{b \in [n]} A_{b\ell}^* z_b^t + \sum_{b \in [n]} A_{b\ell}^* \Delta z_{b \rightarrow \ell}^t \right) \\ &- \mathcal{I}(A_{a\ell}^* z_a^t) \partial_2 \eta^R \left( \sum_{b \in [n]} A_{b\ell}^* z_b^t + \sum_{b \in [n]} A_{b\ell}^* \Delta z_{b \rightarrow \ell}^t \right) \\ &- \mathcal{R}(A_{a\ell}^* z_a^t) \partial_1 \eta^I \left( \sum_{b \in [n]} A_{b\ell}^* z_b^t + \sum_{b \in [n]} A_{b\ell}^* \Delta z_{b \rightarrow \ell}^t \right) \\ &- \mathcal{I}(A_{a\ell}^* z_a^t) \partial_2 \eta^I \left( \sum_{b \in [n]} A_{b\ell}^* z_b^t + \sum_{b \in [n]} A_{b\ell}^* \Delta z_{b \rightarrow \ell}^t \right). \end{aligned} \quad (16)$$

Also, according to (14)

$$z_a^t = y_a - \sum_j A_{aj} x_j^t - \sum_j A_{aj} \Delta x_{j \rightarrow a}^t. \quad (17)$$

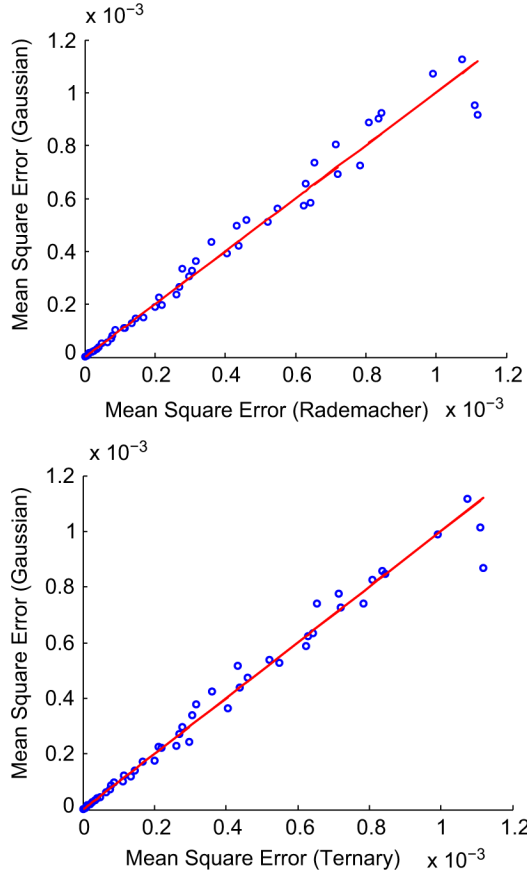


Fig. 8. Comparison of the MSE of c-LASSO for Gaussian and Rademacher matrix ensembles (top), and Gaussian and Ternary ensemble (bottom). The concentration of the points around the  $y = x$  line confirms the universality hypothesis. The norms of residuals are  $2.8 \times 10^{-4}$  and  $2.3 \times 10^{-4}$  for the top and bottom figures respectively. Comparison of this figure with Fig. 6 confirms that as  $N$  grows, the data points concentrate more around  $y = x$  line.

By plugging (16) into (17), we obtain

$$\begin{aligned} & - \sum_j A_{aj} \Delta x_{j \rightarrow a}^t \\ &= \sum_j A_{aj} \mathcal{R}(A_{aj}^* z_a^t) \partial_1 \eta^R \left( \sum_b A_{bj}^* z_b^t + x_j^t \right) \\ &+ \sum_j A_{aj} \mathcal{I}(A_{aj}^* z_a^t) \partial_2 \eta^R \left( \sum_b A_{bj}^* z_b^t + x_j^t \right) \\ &+ i \sum_j A_{aj} \mathcal{R}(A_{aj}^* z_a^t) \partial_1 \eta^I \left( \sum_b A_{bj}^* z_b^t + x_j^t \right) \\ &+ i \sum_j A_{aj} \mathcal{I}(A_{aj}^* z_a^t) \partial_2 \eta^I \left( \sum_b A_{bj}^* z_b^t + x_j^t \right) \end{aligned}$$

which completes the proof.  $\square$

### C. Proof of Lemma III.2

Let  $\mu$  and  $\theta$  denote the amplitude and phase of the random variable  $X$ , respectively. Define  $\nu \triangleq \sqrt{n\pi} = \sqrt{\sigma^2 + \frac{m}{\delta}}$  and  $\zeta \triangleq \frac{\mu}{\nu}$ . Then

$$\begin{aligned} \Psi(m) &= \mathbb{E}|\eta(X + \sqrt{n\pi}Z_1 + i\sqrt{n\pi}Z_2; \tau\sqrt{n\pi}) - X|^2 \\ &= \nu^2 \mathbb{E} \left| \eta \left( \frac{X}{\nu} + Z_1 + iZ_2; \tau \right) - \frac{X}{\nu} \right|^2 \\ &= (1 - \epsilon)\nu^2 \mathbb{E}|\eta(Z_1 + iZ_2; \tau)|^2 \\ &\quad + \epsilon\nu^2 \mathbb{E} (\mathbb{E}_{\zeta, \theta} |\eta(\zeta e^{i\theta} + Z_1 + iZ_2; \tau) - \zeta e^{i\theta}|^2) \quad (18) \end{aligned}$$

where  $\mathbb{E}_{\zeta, \theta}$  denotes the conditional expectation given the variables  $\zeta, \theta$ . Note that the marginal distribution of  $\zeta$  depends only on the marginal distribution of  $\mu$ . The first term in (18) is independent of the phase  $\theta$ , and therefore, we should prove that the second term is also independent of  $\theta$ . Define

$$\Phi(\zeta, \theta) \triangleq \mathbb{E}_{\zeta, \theta}(|\eta(\zeta e^{i\theta} + Z_1 + iZ_2; \tau) - \zeta e^{i\theta}|^2). \quad (19)$$

We prove that  $\Phi$  is independent of  $\theta$ . For two real-valued variables  $z_r$  and  $z_c$ , define  $\mathbf{z} \triangleq (z_r, z_c)$ ,  $d\mathbf{z} \triangleq dz_r dz_c$ , and

$$\begin{aligned} \alpha_z &\triangleq \sqrt{(\zeta \cos \theta + z_r)^2 + (\zeta \sin \theta + z_c)^2} \\ \chi_z &\triangleq \arctan \left( \frac{\zeta \sin \theta + z_c}{\zeta \cos \theta + z_r} \right) \\ c_r &\triangleq \frac{\zeta \cos \theta + z_r}{\alpha_z} \\ c_i &\triangleq \frac{\zeta \sin \theta + z_c}{\alpha_z}. \end{aligned}$$

Define the two sets  $S_\tau \triangleq \{(z_r, z_c) \mid \alpha_z < \tau\}$  and  $S_\tau^c \triangleq \mathbb{R}^2 \setminus S_\tau$ , where “\” is the set subtraction operator. We have

$$\begin{aligned} \Phi(\zeta, \theta) &= \int_{\mathbf{z} \in S_\tau} \zeta^2 \frac{1}{\pi} e^{-(z_r^2 + z_c^2)} d\mathbf{z} \\ &\quad + \int_{\mathbf{z} \in S_\tau^c} |(\alpha_z - \tau)e^{i\chi_z} - \zeta \cos \theta - i\zeta \sin \theta|^2 \frac{1}{\pi} e^{-(z_r^2 + z_c^2)} d\mathbf{z} \\ &= \int_{\mathbf{z} \in S_\tau} \zeta^2 \frac{1}{\pi} e^{-(z_r^2 + z_c^2)} d\mathbf{z} \\ &\quad + \int_{\mathbf{z} \in S_\tau^c} |z_r + iz_c - \tau c_r - i\tau c_i|^2 \frac{1}{\pi} e^{-(z_r^2 + z_c^2)} d\mathbf{z}. \quad (20) \end{aligned}$$

The first integral in (20) corresponds to the case  $|\zeta e^{i\theta} + z_r + iz_c| < \tau$ . The second integral is over the values of  $z_r$  and  $z_c$  for which  $|\zeta e^{i\theta} + z_r + iz_c| \geq \tau$ . Define  $\beta \triangleq \zeta \cos \theta + z_r$  and  $\gamma \triangleq \zeta \sin \theta + z_c$ . We then obtain

$$\begin{aligned} & \int_{\mathbf{z} \in S_\tau^c} |z_r + iz_c - \tau c_r - i\tau c_i|^2 \frac{1}{\pi} e^{-(z_r^2 + z_c^2)} dz_r dz_c \\ &= \int_{\sqrt{\beta^2 + \gamma^2} > \tau} \left| \beta - \zeta \cos \theta + i(\gamma - \zeta \sin \theta) \right. \\ &\quad \left. - \frac{\tau \beta}{\sqrt{\beta^2 + \gamma^2}} - i \frac{\tau \gamma}{\sqrt{\beta^2 + \gamma^2}} \right|^2 \\ &\quad \frac{1}{\pi} e^{-(\beta - \zeta \cos \theta)^2 - (\gamma - \zeta \sin \theta)^2} d\beta d\gamma \\ &\stackrel{(a)}{=} \int_{\phi=0}^{2\pi} \int_{r>\tau} |(r - \tau) \cos \phi - \zeta \cos \theta \\ &\quad + i((r - \tau) \sin \phi - \zeta \sin \theta)|^2 \\ &\quad \frac{1}{\pi} e^{-(r \cos \phi - \zeta \cos \theta)^2 - (r \sin \phi - \zeta \sin \theta)^2} r dr d\phi \\ &= \int_{\phi=0}^{2\pi} \int_{r>\tau} [(r - \tau)^2 + \zeta^2 - 2\zeta(r - \tau) \cos(\theta - \phi)] \\ &\quad e^{-r^2 - \zeta^2 + 2r\zeta \cos(\theta - \phi)} r dr d\phi. \end{aligned}$$

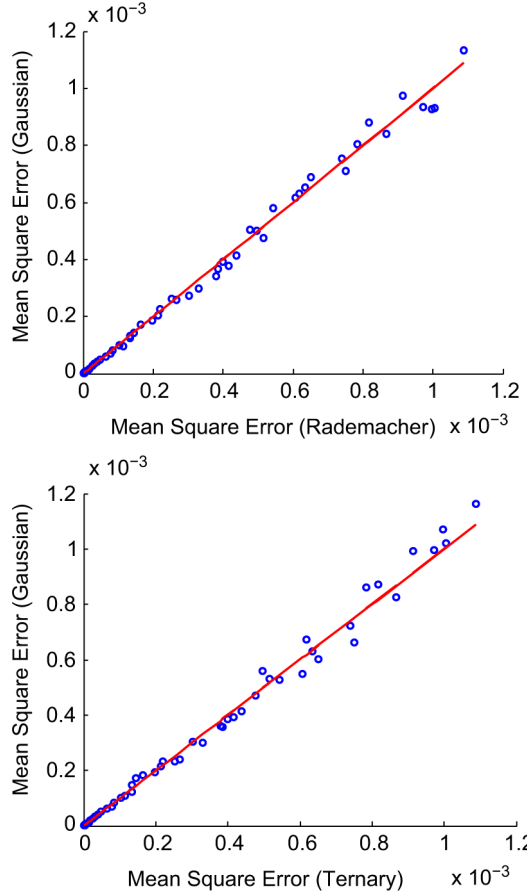


Fig. 9. Comparison of the MSE of CAMP for Gaussian and Rademacher matrix ensembles (top), and Gaussian and Ternary ensemble (bottom). The norms of residuals are  $2 \times 10^{-4}$  and  $1.8 \times 10^{-4}$ , respectively. Comparison with Fig. 7 confirms that as  $N$  grows, the data points concentrate more around  $y = x$  line.

Equality (a) is the result of the change of integration variables from  $\gamma$  and  $\beta$  to  $r \triangleq \sqrt{\beta^2 + \gamma^2}$  and  $\phi \triangleq \arctan\left(\frac{\gamma}{\beta}\right)$ . The periodicity of the cosine function proves that the last integration is independent of the phase  $\theta$ . We can similarly prove that  $\int_{z \in S_\tau} \zeta^2 \frac{1}{\pi} e^{-z_r^2 + z_c^2} dz$  is independent of  $\theta$ . This completes the proof.  $\square$

#### D. Proof of Theorem III.5

We first prove the following lemma that simplifies the proof of Theorem III.5.

**Lemma V.2:** The function  $\Psi(m)$  is concave with respect to  $m$ .

*Proof:* For the notational simplicity define  $\nu \triangleq \sqrt{\sigma^2 + \frac{m}{\delta}}$ ,  $X_\nu \triangleq \frac{X}{\nu}$ , and  $A_\nu \triangleq |X_\nu - Z_1 + iZ_2|$ . We note that

$$\begin{aligned} \frac{d^2\Psi}{dm^2} &= \frac{d}{dm} \left( \frac{d\Psi}{dm} \right) = \frac{d}{dm} \left( \frac{d\Psi}{d(\nu^2)} \frac{d\nu^2}{dm} \right) \\ &= \frac{1}{\delta} \frac{d}{dm} \left( \frac{d\Psi}{d\nu^2} \right) = \frac{1}{\delta^2} \frac{d^2\Psi}{d(\nu^2)^2}. \end{aligned}$$

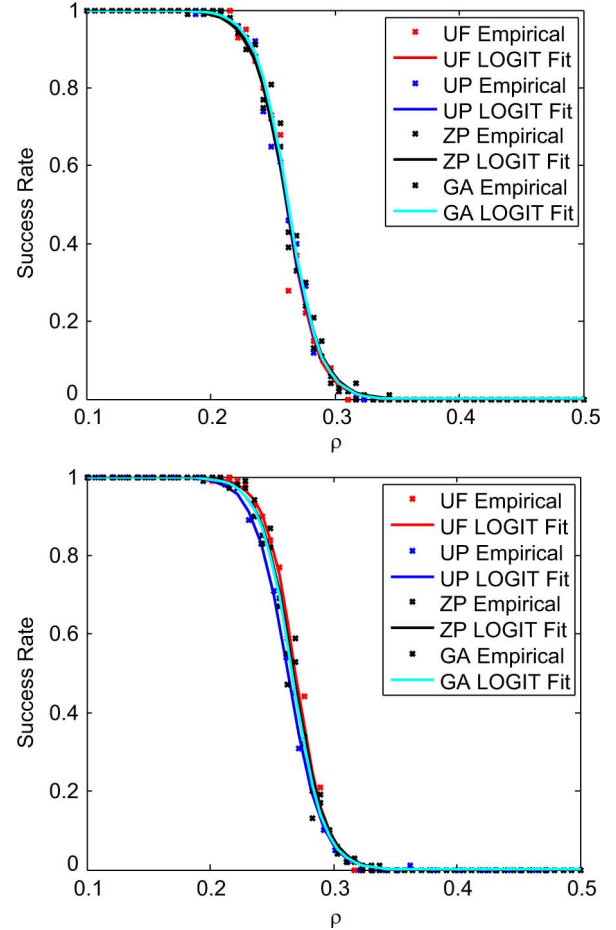


Fig. 10. Comparison of the phase transition of c-LASSO (top) and CAMP (bottom) for different coefficient ensembles specified in Table II.  $\delta = 0.1$  in this figure. These figures are in agreement with Proposition III.4 that claims that the phase transitions of CAMP and c-LASSO are independent of the distribution of the nonzero coefficients. Simulations at other values of  $\delta$  result in similar behavior.

Therefore,  $\Psi$  is concave with respect to  $m$  if and only if it is concave with respect to  $\nu^2$ . According to Lemma III.2, the phase distribution of  $X$  does not affect the  $\Psi$  function. Therefore, we set the phase of  $X$  to zero and assume that it is a positive-valued random variable (representing the amplitude). This assumption substantially simplifies the calculations. We have

$$\begin{aligned} \Psi(\nu^2) &= \nu^2 \mathbb{E} \left( |\eta(X_\nu + Z_1 + iZ_2; \tau) - X_\nu|^2 \right) \\ &= \nu^2 \mathbb{E} \left( \mathbb{E}_X \left( |\eta(X_\nu + Z_1 + iZ_2; \tau) - X_\nu|^2 \right) \right) \end{aligned}$$

where  $\mathbb{E}_X$  denotes the expected value conditioned on the random variable  $X$ . We first prove that  $\Psi_X(\nu^2) \triangleq \nu^2 \mathbb{E}_X \left( |\eta(X_\nu + Z_1 + iZ_2; \tau) - X_\nu|^2 \right)$  is concave with respect to  $\nu^2$  by proving  $\frac{d\Psi_X}{d(\nu^2)^2} \leq 0$ . Then, since  $\Psi(\nu^2)$  is a convex combination of  $\Psi_X(\nu^2)$ , we conclude that  $\Psi(\nu^2)$  is a concave function of  $\nu^2$  as well. The rest of the proof details the algebra required for calculating and simplifying  $\frac{d^2\Psi_X}{d\nu^2}$ .

Using the real and imaginary parts of the soft thresholding function and its partial derivatives introduced in (12) and (13), we have

$$\begin{aligned} \frac{d\Psi_X(\nu^2)}{d\nu^2} &= \mathbb{E}_X |\eta(X_\nu + Z_1 + iZ_2; \tau) - X_\nu|^2 \\ &\quad + \nu^2 \frac{d}{d\nu} \mathbb{E}_X |\eta(X_\nu + Z_1 + iZ_2; \tau) - X_\nu|^2 \frac{d\nu}{d(\nu^2)} \\ &= \mathbb{E}_X |\eta(X_\nu + Z_1 + iZ_2; \tau) - X_\nu|^2 \\ &\quad + \frac{\nu}{2} \frac{d}{d\nu} \mathbb{E}_X |\eta(X_\nu + Z_1 + iZ_2; \tau) - X_\nu|^2 \\ &= \mathbb{E}_X |\eta(X_\nu + Z_1 + iZ_2; \tau) - X_\nu|^2 \\ &\quad - X_\nu \mathbb{E}_X \left[ (\partial_1 \eta^R(X_\nu + Z_1 + iZ_2; \tau) - 1) \right. \\ &\quad \left. (\eta^R(X_\nu + Z_1 + iZ_2; \tau) - X_\nu) \right] \\ &\quad - X_\nu \mathbb{E}_X \left[ (\partial_1 \eta^I(X_\nu + Z_1 + iZ_2; \tau)) \right. \\ &\quad \left. (\eta^I(X_\nu + Z_1 + iZ_2; \tau)) \right] \end{aligned}$$

where  $\partial_1^R, \partial_2^R, \partial_1^I$ , and  $\partial_2^I$  are defined in (13). Note that in the above calculations,  $\partial_2 \eta^R$  and  $\partial_2 \eta^I$  did not appear, since we assumed that  $X$  is a real-valued random variable. Define  $A_\nu \triangleq \sqrt{(X_\nu + Z_1)^2 + Z_2^2}$ . It is straightforward to show that

$$\begin{aligned} \partial_1 \eta^R(X_\nu + Z_1 + iZ_2; \tau) &= \left(1 - \frac{\tau Z_2^2}{A_\nu^3}\right) \mathbb{I}(A_\nu > \tau) \\ \eta^R(X_\nu + Z_1 + iZ_2; \tau) &= (X_\nu + Z_1) \left(1 - \frac{\tau}{A_\nu}\right) \mathbb{I}(A_\nu \geq \tau) \\ \partial_1 \eta^I(X_\nu + Z_1 + iZ_2; \tau) &= \frac{\tau(X_\nu + Z_1)Z_2}{A_\nu^3} \mathbb{I}(A_\nu \geq \tau) \\ \eta^I(X_\nu + Z_1 + iZ_2; \tau) &= \left(Z_2 - \frac{\tau Z_2}{A_\nu}\right) \mathbb{I}(A_\nu \geq \tau). \quad (21) \end{aligned}$$

For  $f : \mathbb{C} \rightarrow \mathbb{R}$ , we define  $\partial_1^2 f(x + iy) \triangleq \frac{\partial^2 f(x+iy)}{\partial x^2}$ . It is straightforward to show that

$$\begin{aligned} \frac{d^2 \Psi_X(\nu^2)}{d^2 \nu^2} &= -\frac{X}{\nu^3} \mathbb{E}_X \left[ (\partial_1 \eta^R(X_\nu + Z_1 + iZ_2; \tau) - 1) \right. \\ &\quad \left. (\eta^R(X_\nu + Z_1 + iZ_2; \tau) - X_\nu) \right] \\ &\quad - \frac{X}{\nu^3} \mathbb{E}_X \left[ (\partial_1 \eta^I(X_\nu + Z_1 + iZ_2; \tau)) \right. \\ &\quad \left. (\eta^I(X_\nu + Z_1 + iZ_2; \tau)) \right] \\ &\quad + \frac{X}{2\nu^3} \mathbb{E}_X \left[ (\partial_1 \eta^R(X_\nu + Z_1 + iZ_2; \tau) - 1) \right. \\ &\quad \left. (\eta^R(X_\nu + Z_1 + iZ_2; \tau) - X_\nu) \right] \\ &\quad + \frac{X}{2\nu^3} \mathbb{E}_X \left[ (\partial_1 \eta^I(X_\nu + Z_1 + iZ_2; \tau)) \right. \\ &\quad \left. (\eta^I(X_\nu + Z_1 + iZ_2; \tau)) \right] \\ &\quad + \frac{X^2}{2\nu^4} \mathbb{E}_X (\partial_1 \eta^R(X_\nu + Z_1 + iZ_2; \tau) - 1)^2 \end{aligned}$$

$$\begin{aligned} &+ \frac{X^2}{2\nu^4} \mathbb{E}_X (\partial_1 \eta^I(X_\nu + Z_1 + iZ_2; \tau))^2 \\ &+ \frac{X^2}{2\nu^4} \mathbb{E}_X \left[ (\partial_1^2 \eta^R(X_\nu + Z_1 + iZ_2; \tau)) \right. \\ &\quad \left. (\eta^R(X_\nu + Z_1 + iZ_2; \tau) - X_\nu) \right] \\ &+ \frac{X^2}{2\nu^4} \mathbb{E}_X \left[ (\partial_1^2 \eta^I(X_\nu + Z_1 + iZ_2; \tau)) \right. \\ &\quad \left. (\eta^I(X_\nu + Z_1 + iZ_2; \tau)) \right]. \quad (22) \end{aligned}$$

Our next objective is to simplify the terms in (22). We start with

$$\begin{aligned} &\mathbb{E}_X \left[ (\partial_1 \eta^R(X_\nu + Z_1 + iZ_2; \tau) - 1) \right. \\ &\quad \left. (\eta^R(X_\nu + Z_1 + iZ_2; \tau) - X_\nu) \right] \\ &+ \mathbb{E}_X \left[ (\partial_1 \eta^I(X_\nu + Z_1 + iZ_2; \tau)) \right. \\ &\quad \left. (\eta^I(X_\nu + Z_1 + iZ_2; \tau)) \right] \\ &= \frac{X}{\nu} \mathbb{E}_X \left( \mathbb{I}(A_\nu \leq \tau) + \frac{\tau Z_2^2}{A_\nu^3} \mathbb{I}(A_\nu \geq \tau) \right). \quad (23) \end{aligned}$$

Similarly

$$\begin{aligned} &\mathbb{E}_X (\partial_1 \eta^R(X_\nu + Z_1 + iZ_2; \tau) - 1)^2 \\ &+ \mathbb{E}_X (\partial_1 \eta^I(X_\nu + Z_1 + iZ_2; \tau))^2 \\ &= \mathbb{E}_X \left( \left(1 - \frac{\tau Z_2^2}{A_\nu^3}\right) \mathbb{I}(A_\nu \geq \tau) - 1 \right)^2 \\ &+ \mathbb{E} \left( \frac{\tau(X_\nu + Z_1)Z_2}{A_\nu^3} \mathbb{I}(A_\nu \geq \tau) \right)^2 \\ &= \mathbb{E}_X \left( \mathbb{I}(A_\nu \leq \tau) + \frac{\tau^2 Z_2^4}{A_\nu^6} \mathbb{I}(A_\nu \geq \tau) \right) \\ &+ \mathbb{E}_X \left( \frac{\tau^2(X_\nu + Z_1)^2 Z_2^2}{A_\nu^6} \mathbb{I}(A_\nu \geq \tau) \right) \\ &= \mathbb{E}_X \left( \mathbb{I}(A_\nu \leq \tau) + \frac{\tau^2 Z_2^2}{A_\nu^4} \mathbb{I}(A_\nu \geq \tau) \right). \quad (24) \end{aligned}$$

We also have

$$\begin{aligned} &\partial_1^2 \eta^R(X_\nu + Z_1 + iZ_2; \tau) \\ &= \frac{3\tau Z_2^2 (X_\nu + Z_1)}{A_\nu^5} \mathbb{I}(A_\nu \geq \tau) \\ &+ \left(1 - \frac{\tau Z_2^2}{A_\nu^3}\right) \left(\frac{X_\nu + Z_1}{A_\nu}\right) \delta(A_\nu - \tau) \end{aligned}$$

and

$$\begin{aligned} &\partial_1^2 \eta^I(X_\nu + Z_1 + iZ_2; \tau) \\ &= \frac{\tau Z_2}{A_\nu^3} \mathbb{I}(A_\nu \geq \tau) \\ &- 3\tau \frac{(X_\nu + Z_1)^2 Z_2}{A_\nu^5} \mathbb{I}(A_\nu \geq \tau) \\ &+ \frac{\tau(X_\nu + Z_1)^2 Z_2}{A_\nu^4} \delta(A_\nu - \tau). \end{aligned}$$

Define

$$\begin{aligned} S &\stackrel{\Delta}{=} \mathbb{E}_X \left[ (\partial_1^2 \eta^R(X_\nu + Z_1 + iZ_2; \tau)) \right. \\ &\quad \left. (\eta^R(X_\nu + Z_1 + iZ_2; \tau) - X_\nu) \right] \\ &+ \mathbb{E}_X \left[ \partial_1^2 \eta^I(X_\nu + Z_1 + iZ_2; \tau) \right. \\ &\quad \left. \eta^I(X_\nu + Z_1 + iZ_2; \tau) \right]. \end{aligned}$$

We then have

$$\begin{aligned} S &= \mathbb{E}_X \left( \frac{3\tau Z_1 Z_2^2 (X_\nu + Z_1)}{A_\nu^5} \mathbb{I}(A_\nu \geq \tau) \right) \\ &- \mathbb{E}_X \left( \frac{3\tau^2 (X_\nu + Z_1)^2 Z_2^2}{A_\nu^6} \mathbb{I}(A_\nu \geq \tau) \right) \\ &- \mathbb{E}_X \left( \frac{X_\nu (X_\nu + Z_1)}{A_\nu} \left( 1 - \frac{Z_2^2}{A_\nu^2} \right) \delta(A_\nu - \tau) \right) \\ &+ \mathbb{E}_X \left( \left( \frac{\tau Z_2^2}{A_\nu^3} - \frac{\tau^2 Z_2^2}{A_\nu^4} \right) \mathbb{I}(A_\nu \geq \tau) \right) \\ &- \mathbb{E}_X \left( \frac{3\tau (X_\nu + Z_1)^2 Z_2^2}{A_\nu^5} \mathbb{I}(A_\nu \geq \tau) \right) \\ &- \mathbb{E}_X \left( \frac{3\tau^2 (X_\nu + Z_1)^2 Z_2^2}{A_\nu^6} \mathbb{I}(A_\nu \geq \tau) \right). \end{aligned}$$

Note that in the above expression, we have replaced  $\left(1 - \frac{\tau Z_2^2}{A_\nu^3}\right) \delta(A_\nu - \tau)$  with  $\left(1 - \frac{Z_2^2}{A_\nu^2}\right) \delta(A_\nu - \tau)$  for an obvious reason. It is straightforward to simplify this expression to obtain

$$\begin{aligned} S &= \mathbb{E}_X \left( \left( \frac{\tau Z_2^2}{A_\nu^3} - \frac{\tau^2 Z_2^2}{A_\nu^4} \right) \mathbb{I}(A_\nu \geq \tau) \right) \\ &- \mathbb{E}_X \left( \left( \frac{3\tau (X_\nu + Z_1) Z_2^2 X_\nu}{A_\nu^5} \right) \mathbb{I}(A_\nu \geq \tau) \right) \\ &- \mathbb{E}_X \left( \frac{X_\nu (X_\nu + Z_1)}{A_\nu} \left( 1 - \frac{Z_2^2}{A_\nu^2} \right) \delta(A_\nu - \tau) \right). \end{aligned} \quad (25)$$

By plugging (23), (24), and (25) into (22), we obtain

$$\begin{aligned} \frac{d^2 \Psi_X(\nu^2)}{d^2 \nu^2} &= -\mathbb{E} \frac{3\tau X^3 (X_\nu + Z_1) Z_2^2}{2\nu^5 A_\nu^5} \mathbb{I}(A_\nu \geq \tau) \\ &- \mathbb{E} \left( \frac{X_\nu (X_\nu + Z_1)}{A_\nu} \right) \left( 1 - \frac{Z_2^2}{A_\nu^2} \right) \delta(A_\nu - \tau). \end{aligned} \quad (26)$$

We claim that both terms on the right hand side of (26) are negative. To prove this claim, we first focus on the first term:

$$\mathbb{E} \left( \frac{(X_\nu + Z_1) Z_2^2}{A_\nu^5} \mathbb{I}(A_\nu \geq \tau) \right) \geq 0.$$

Define  $S_\tau \stackrel{\Delta}{=} \{(Z_1, Z_2) \mid A_\nu \geq \tau\}$ . We have

$$\begin{aligned} &\mathbb{E} \left( \frac{(X_\nu + Z_1) Z_2^2}{A_\nu^5} \mathbb{I}(A_\nu \geq \tau) \right) \\ &= \int \int_{(z_1, z_2) \in S_\tau} \frac{(X_\nu + z_1) z_2^2}{A_\nu^5} \frac{1}{\pi} e^{-z_1^2 - z_2^2} dz_1 dz_2 \\ &\stackrel{(a)}{=} \int_\tau^\infty \int_0^{2\pi} \frac{r \cos \phi r^2 \sin^2 \phi e^{-r^2 - X_\nu^2 + 2r X_\nu \cos \phi}}{r^5} r d\phi dr \\ &= \int_\tau^\infty \int_0^{2\pi} \frac{\sin^2 \phi e^{-r^2 - X_\nu^2 + 2r X_\nu \cos \phi}}{r} d\sin(\phi) dr \geq 0. \end{aligned} \quad (27)$$

Equality (a) is the result of the change of integration variables from  $z_1, z_2$  to  $r \stackrel{\Delta}{=} A_\nu$  and  $\phi \stackrel{\Delta}{=} \arctan \left( \frac{z_2}{z_1 + X_\nu} \right)$ . With exactly similar approach, we can prove that the second term of (26) is also negative.

So far we have proved that  $\Psi_X(m)$  is concave with respect to  $m$ . But this implies that  $\Psi(m)$  is also concave, since it is a convex combination of concave functions. ■

*Proof of Theorem III.5:* As proved in Lemma V.2,  $\Psi(m)$  is a concave function. Furthermore  $\Psi(0) = 0$ . Therefore a given value of  $\rho$  is below the phase transition, i.e.,  $\rho < \rho_{SE}(\delta)$  if and only if  $\frac{d\Psi}{dm}|_m < 1$ . It is straightforward to calculate the derivative at zero and confirm that

$$\frac{d\Psi}{dm} \Big|_{m=0} = \frac{\rho \delta (1 + \tau^2)}{\delta} + \frac{1 - \rho \delta}{\delta} \mathbb{E} |\eta(Z_1 + iZ_2; \tau)|^2. \quad (28)$$

Since  $Z_1, Z_2 \sim N(0, 1/2)$  and are independent, the phase of  $Z_1 + iZ_2$  has a uniform distribution, while its amplitude has Rayleigh distribution. Therefore, we have

$$\mathbb{E} |\eta(Z_1 + iZ_2; \tau)|^2 = 2 \int_\tau^\infty \omega (\omega - \tau)^2 e^{-\omega^2} d\omega. \quad (29)$$

We plug (29) into (28) and set the derivative  $\frac{d\Psi}{dm}|_m = 1$  to obtain the value of  $\rho$  at which the phase transition occurs. This value is given by

$$\rho = \frac{\delta - 2 \int_\tau^\infty \omega (\omega - \tau)^2 e^{-\omega^2} d\omega}{\delta (1 + \tau^2) - 2 \int_\tau^\infty \omega (\omega - \tau)^2 e^{-\omega^2} d\omega}.$$

Clearly the phase transition depends on  $\tau$ . Hence, according to the framework we introduced in Section I-D1, we search for the value of  $\tau$  that maximizes the phase transition  $\rho$ . Define  $\chi_1(\tau) \stackrel{\Delta}{=} \int_{\tau_*}^\infty \omega (\tau_* - \omega) e^{-\omega^2} d\omega$  and  $\chi_2(\tau) \stackrel{\Delta}{=} \int_{\tau_*}^\infty \omega (\omega - \tau)^2 e^{-\omega^2} d\omega$ . This optimal  $\tau$  satisfies

$$\begin{aligned} &4\chi_1(\tau^*) (1 + \tau_*^2 - 2\chi_2(\tau^*)) \\ &= (4\chi_1(\tau^*) - 2\tau_*) (\delta - 2\chi_2(\tau^*)) \end{aligned}$$

which, in turn, results in  $\delta = \frac{4(1+\tau^2)\chi_1(\tau^*) - 4\tau_*\chi_2(\tau^*)}{-2\tau_* + 4\chi_1(\tau^*)}$ . Plugging  $\delta$  into the formula for  $\rho$ , we obtain the formula in Theorem III.5. ■

### E. Proof of Theorem III.6

We first show that the value of  $\delta$  in Theorem III.5 goes to zero as  $\tau \rightarrow \infty$ . By changing the variable of integration from  $\omega$  to  $\gamma = \omega - \tau$ , we obtain

$$\begin{aligned} \left| \int_{\omega \geq \tau} \omega(\omega - \tau) e^{-\omega^2} d\omega \right| &= \left| \int_{\gamma \geq 0} (\gamma + \tau) \gamma e^{-(\gamma + \tau)^2} d\gamma \right| \\ &\leq \left| e^{-\tau^2} \int_{\gamma \geq 0} (\gamma + \tau) \gamma e^{-\gamma^2} d\gamma \right| \\ &= e^{-\tau^2} \left( \frac{1}{4} + \frac{\tau}{2\sqrt{\pi}} \right). \end{aligned} \quad (30)$$

Again by changing integration variables, we have

$$\begin{aligned} \left| \int_{\omega \geq \tau} \omega(\omega - \tau)^2 e^{-\omega^2} d\omega \right| &= \left| \int_{\gamma \geq 0} (\gamma + \tau) \gamma^2 e^{-(\gamma + \tau)^2} d\gamma \right| \\ &\leq e^{-\tau^2} \int_{\gamma > 0} (\gamma + \tau) \gamma^2 e^{-\gamma^2} d\gamma \\ &= e^{-\tau^2} \left( \frac{\tau}{4} + \frac{1}{2\sqrt{\pi}} \right). \end{aligned} \quad (31)$$

Using (30) and (31) in the formula for  $\delta$  in Theorem III.5 establishes that  $\delta \rightarrow 0$  as  $\tau \rightarrow \infty$ . Therefore, in order to find the asymptotic behavior of the phase transition as  $\delta \rightarrow 0$ , we can calculate the asymptotic behavior of  $\delta$  and  $\rho$  as  $\tau \rightarrow \infty$ . This is a standard application of Laplace's method. Using this method, we calculate the leading terms of  $\rho$  and  $\delta$ :

$$\int_{\tau}^{\infty} \omega(\tau - \omega) e^{-\omega^2} d\omega \sim \frac{e^{-\tau^2}}{8\tau^3}, \quad \tau \rightarrow \infty \quad (32)$$

$$\int_{\tau}^{\infty} \omega(\tau - \omega)^2 e^{-\omega^2} d\omega \sim \frac{e^{-\tau^2}}{4\tau^2}, \quad \tau \rightarrow \infty. \quad (33)$$

Plugging (32) and (33) into the formula we have for  $\rho$  and  $\delta$  in Theorem III.5, we obtain

$$\delta \sim \frac{e^{-\tau^2}}{2}, \quad \tau \rightarrow \infty$$

$$\rho \sim \frac{1}{\tau^2}, \quad \tau \rightarrow \infty$$

which completes the proof.  $\square$

### F. Proof of Lemma III.7

According to Lemma III.2, the phase  $\theta$  does not affect the risk function, and therefore we set it to zero. We have

$$\begin{aligned} r(\mu, \tau) &= \mathbb{E} |\eta(\mu + Z_1 + iZ_2; \tau) - \mu|^2 \\ &= \mathbb{E}(\eta^R(\mu + Z_1 + iZ_2; \tau) - \mu)^2 \\ &\quad + \mathbb{E}(\eta^I(\mu + Z_1 + iZ_2; \tau))^2 \end{aligned}$$

where  $\eta^R(\mu + Z_1 + iZ_2; \tau) = \left( \mu + Z_1 - \frac{\tau(\mu + Z_1)}{A} \right) \mathbb{I}(A \geq \tau)$ ,  $\eta^I(\mu + Z_1 + iZ_2; \tau) = (z_2 - \frac{\tau z_2}{A}) \mathbb{I}(A \geq \tau)$ , and  $A \triangleq \sqrt{(\mu + Z_1)^2 + Z_2^2}$ . If we calculate the derivative of the risk function with respect to  $\mu$ , then we have

$$\begin{aligned} \frac{dr(\mu, \tau)}{d\mu} &= 2\mathbb{E}(\eta^R(\mu + Z_1 + iZ_2; \tau) - \mu) \left( \frac{d\eta^R}{d\mu} - 1 \right) \\ &\quad + 2\mathbb{E}\eta^I(\mu + Z_1 + iZ_2; \tau) \frac{d\eta^I}{d\mu}. \end{aligned}$$

It is straightforward to show that

$$\begin{aligned} \frac{dr(\mu, \tau)}{d\mu} &= \mathbb{E} \left[ (\eta^R(\mu + Z_1 + iZ_2; \tau) - \mu) \right. \\ &\quad \left. \left( \left( 1 - \frac{\tau Z_2^2}{A^3} \right) \mathbb{I}(A \geq \tau) - 1 \right) \right] \\ &+ \mathbb{E} \left[ \eta^I(\mu + Z_1 + iZ_2; \tau) \left( \frac{\tau(\mu + Z_1) Z_2}{A^3} \right) \mathbb{I}(A \geq \tau) \right] \\ &= \mu \mathbb{E}[\mathbb{I}(A \leq \tau)] \\ &- \mathbb{E} \left[ \left( Z_1 - \frac{\tau(\mu + Z_1)}{A} \right) \left( \frac{\tau Z_2^2}{A^3} \right) \mathbb{I}(A \geq \tau) \right] \\ &+ \mathbb{E} \left[ \left( Z_2 - \frac{\tau Z_2}{A} \right) \left( \frac{\tau(\mu + Z_1) Z_2}{A^3} \right) \mathbb{I}(A \geq \tau) \right] \\ &= \mu \mathbb{E}[\mathbb{I}(A \leq \tau)] \\ &- \mathbb{E} \left[ \left( \frac{\tau Z_1 Z_2^2}{A^3} + \frac{\tau^2 \mu Z_2^2}{A^4} + \frac{\tau^2 Z_1 Z_2^2}{A^4} \right) \mathbb{I}(A \geq \tau) \right] \\ &+ \mathbb{E} \left[ \left( \frac{\tau \mu Z_2^2}{A^3} + \frac{\tau Z_2^2 Z_1}{A^3} - \frac{\tau^2 \mu Z_2^2}{A^4} - \frac{\tau^2 Z_1 Z_2}{A^4} \right) \mathbb{I}(A \geq \tau) \right] \\ &= \mu \mathbb{E}[\mathbb{I}(A \leq \tau)] + \mu \mathbb{E} \left[ \frac{\tau Z_2^2}{A^3} \right] \geq 0. \end{aligned}$$

Therefore, the risk of the complex soft thresholding is an increasing function of  $\mu$ . Furthermore

$$2 \frac{dr(\mu, \tau)}{d\mu^2} = \frac{1}{\mu} \frac{dr(\mu, \tau)}{d\mu} = \mathbb{E}(\mathbb{I}(A \leq \tau)) + \mathbb{E} \left( \frac{\tau Z_2^2}{A^3} \right).$$

It is clear that the next derivative with respect to  $\mu^2$  is negative, and therefore, the function is concave.  $\square$

### G. Proof of Proposition III.8

As is clear from the statement of the theorem, the main challenge here is to characterize

$$\sup_{q \in F_\epsilon} \mathbb{E}|\eta(X + Z_1 + iZ_2; \tau) - X|^2.$$

Let  $X = \mu e^{i\theta}$ , where  $\mu$  and  $\theta$  are the phase and amplitude of  $X$  respectively. According to Lemma III.2, the risk function is independent of  $\theta$ . Furthermore, since  $q \in F_\epsilon$ , we can write it as  $q(\mu) = (1 - \epsilon)\delta_0(\mu) + (1 - \epsilon)G(\mu)$ , where  $G$  is absolutely continuous with respect to Lebesgue measure. We then have

$$\begin{aligned} \mathbb{E}|\eta(\mu + Z_1 + iZ_2; \tau) - X|^2 &= (1 - \epsilon)\mathbb{E}|\eta(Z_1 + iZ_2; \tau)|^2 \\ &\quad + \epsilon \mathbb{E}_{\mu \sim G} \mathbb{E}_X |\eta(\mu + Z_1 + iZ_2; \tau) - \mu|^2 \\ &= 2(1 - \epsilon) \int_{w=\tau}^{\infty} w(w - \tau)^2 e^{-w^2} dw \\ &\quad + \epsilon \mathbb{E}_{\mu \sim G} \mathbb{E}_{\mu} |\eta(\mu + Z_1 + iZ_2; \tau) - \mu|^2. \end{aligned} \quad (34)$$

The notation  $\mathbb{E}_{\mu \sim G_m}$  means that we are taking the expectation with respect to  $\mu$ , whose distribution is  $G$ . Also  $\mathbb{E}_{\mu}$  represents the conditional expectation given the random variable  $\mu$ . Define  $\delta_m(\mu) \triangleq \delta(\mu - m)$ . Using Lemma III.7 and the Jensen inequality, we prove that  $\{G_m(\mu)\}_{m=1}^{\infty}$ ,  $G_m(\mu) = \delta_m(\mu)$  is the least favorable sequence of distributions, i.e., for any distribution  $G$

$$\begin{aligned} \mathbb{E}_{\mu \sim G} \mathbb{E}_{\mu} |\eta(\mu + Z_1 + iZ_2; \tau) - \mu|^2 &\leq \lim_{m \rightarrow \infty} \mathbb{E}_{\mu \sim G_m} \mathbb{E}_{\mu} |\eta(\mu + Z_1 + iZ_2; \tau) - \mu|^2. \end{aligned}$$

Toward this end, we define  $\tilde{G}(\mu)$  as  $\delta_{\mu_0}(\mu)$  such that  $\mu_0^2 = E_G(\mu^2)$ . In other words,  $\tilde{G}$  and  $G$  have the same second moments. From the Jensen inequality, we have

$$\begin{aligned} & \mathbb{E}_{\mu \sim G} \mathbb{E}_\mu |\eta(\mu + Z_1 + iZ_2; \tau) - \mu|^2 \\ & \leq \mathbb{E}_{\mu \sim \tilde{G}} \mathbb{E}_\mu |\eta(\mu + Z_1 + iZ_2; \tau) - \mu|^2. \end{aligned}$$

Furthermore, from the monotonicity of the risk function proved in Lemma III.7, we have

$$\begin{aligned} & \mathbb{E}_{\mu \sim \tilde{G}} \mathbb{E}_\mu |\eta(\mu + Z_1 + iZ_2; \tau) - \mu|^2 \\ & \leq \mathbb{E}_{\mu \sim G_m} \mathbb{E}_\mu |\eta(\mu + Z_1 + iZ_2; \tau) - \mu|^2 \quad \forall m > \mu_0. \end{aligned}$$

Again we can use the monotonicity of the risk function to prove that

$$\begin{aligned} & \mathbb{E}_{\mu \sim G_m} \mathbb{E}_\mu |\eta(\mu + Z_1 + iZ_2; \tau) - \mu|^2 \\ & \leq \lim_{m \rightarrow \infty} \mathbb{E}_{\mu \sim G_m} \mathbb{E}_\mu |\eta(\mu + Z_1 + iZ_2; \tau) - \mu|^2 \\ & = 1 + \tau^2. \end{aligned} \quad (35)$$

The last equality is the result of the monotone convergence theorem. Combining (34) and (35) completes the proof.  $\square$

## VI. CONCLUSION

We have considered the problem of recovering a complex-valued sparse signal from an undersampled set of complex-valued measurements. We have accurately analyzed the asymptotic performance of c-LASSO and CAMP algorithms. Using the SE framework, we have derived simple expressions for the noise sensitivity and phase transition of these two algorithms. The results presented here show that substantial improvements can be achieved when the real and imaginary parts are considered jointly by the recovery algorithm. For instance, Theorem III.6 shows that in the high undersampling regime, the phase transition of CAMP and c-BP is two times higher than the phase transition of r-LASSO.

## ACKNOWLEDGMENT

Thanks to David Donoho and Andrea Montanari for their encouragement and their valuable suggestions on an early draft of this paper. We would also like to thank the reviewers and the associate editor for the thoughtful comments that helped us improve the quality of the manuscript, and to thank Ali Mousavi for careful reading of our paper and suggesting improvements.

## REFERENCES

- [1] J. A. Tropp and S. J. Wright, "Computational methods for sparse solution of linear inverse problems," *Proc. IEEE*, vol. 98, no. 6, pp. 948–958, Jun. 2010.
- [2] S. S. Chen, D. L. Donoho, and M. A. Saunders, "Atomic decomposition by basis pursuit," *SIAM J. Sci. Comput.*, vol. 20, pp. 33–61, 1998.
- [3] D. L. Donoho, A. Maleki, and A. Montanari, "Message passing algorithms for compressed sensing," *Proc. Natl. Acad. Sci.*, vol. 106, no. 45, pp. 18914–18919, 2009.
- [4] E. Van Den Berg and M. P. Friedlander, "Probing the Pareto frontier for basis pursuit solutions," *SIAM J. Sci. Comput.*, vol. 31, no. 2, pp. 890–912, 2008.
- [5] Z. Yang, C. Zhang, J. Deng, and W. Lu, "Orthonormal expansion  $\ell_1$ -minimization algorithms for compressed sensing," Preprint 2010.
- [6] A. Maleki and D. L. Donoho, "Optimally tuned iterative thresholding algorithm for compressed sensing," *IEEE J. Sel. Topics Signal Process.*, Apr. 2010.
- [7] M. Lustig, D. L. Donoho, and J. Pauly, "Sparse MRI: The application of compressed sensing for rapid MR imaging," *Mag. Reson. Med.*, vol. 58, no. 6, pp. 1182–1195, Dec. 2007.
- [8] L. Anitori, A. Maleki, M. Otten, R. G. Baraniuk, and W. Van Rossum, "Compressive CFAR radar detection," in *Proc. IEEE Radar Conf.*, May 2012, pp. 0320–0325.
- [9] R. G. Baraniuk and P. Steeghs, "Compressive radar imaging," in *Proc. IEEE Radar Conf.*, Apr. 2007, pp. 128–133.
- [10] M. A. Herman and T. Strohmer, "High-resolution radar via compressed sensing," *IEEE Trans. Signal Process.*, vol. 57, no. 6, pp. 2275–2284, Jun. 2009.
- [11] D. L. Donoho, A. Maleki, and A. Montanari, "Noise sensitivity phase transition," *IEEE Trans. Inf. Theory*, submitted for publication.
- [12] P. Schniter and J. P. Vila, "Expectation-maximization Gaussian-mixture approximate message passing," Preprint 2012 [Online]. Available: arXiv:1207.3107v1
- [13] S. Som, L. C. Potter, and P. Schniter, "Compressive imaging using approximate message passing and a Markov-tree prior," in *Proc. Asilomar Conf. Signals, Syst., Comput.*, Nov. 2010, pp. 243–247.
- [14] R. Tibshirani, "Regression shrinkage and selection via the Lasso," *J. Roy. Stat. Soc. Ser. B*, vol. 58, no. 1, pp. 267–288, 1996.
- [15] A. Maleki and R. G. Baraniuk, "Least favorable compressed sensing problems for the first order methods," in *Proc. IEEE Int. Symp. Inf. Theory*, 2011, pp. 134–138.
- [16] M. Bayati and A. Montanari, "The dynamics of message passing on dense graphs, with applications to compressed sensing," *IEEE Trans. Inf. Theory*, vol. 57, no. 2, pp. 764–785, Feb. 2011.
- [17] G. Taubock and F. Hlawatsch, "A compressed sensing technique for OFDM channel estimation in mobile environments: Exploiting channel sparsity for reducing pilots," in *Proc. IEEE Int. Conf. Acoust., Speech, Signal Process.*, 2008, pp. 2885–2888.
- [18] J. S. Picard and A. J. Weiss, "Direction finding of multiple emitters by spatial sparsity and linear programming," in *Proc. IEEE Int. Symp. Inf. Theory*, Sep. 2009, pp. 1258–1262.
- [19] D. L. Donoho and J. Tanner, "Precise undersampling theorems," *Proc. IEEE*, vol. 98, no. 6, pp. 913–924, Jun. 2010.
- [20] D. L. Donoho and J. Tanner, "Observed universality of phase transitions in high-dimensional geometry, with applications in modern signal processing and data analysis," *Philos. Trans. Roy. Soc. A*, vol. 367, no. 1906, pp. 4273–4293, 2009.
- [21] M. Figueiredo, R. Nowak, and S. J. Wright, "Gradient projection for sparse reconstruction: Application to compressed sensing and other inverse problems," *IEEE J. Sel. Topics Signal Process.*, vol. 1, no. 4, pp. 586–598, Dec. 2007.
- [22] S. J. Wright, R. Nowak, and M. Figueiredo, "Sparse reconstruction by separable approximation," in *Proc. IEEE Int. Conf. Acoust., Speech, Signal Process.*, 2009, pp. 3373–3376.
- [23] S. J. Kim, K. Koh, M. Lustig, S. Boyd, and D. Gorinevsky, "A method for large-scale  $\ell_1$ -regularized least squares," *IEEE J. Sel. Topics Signal Process.*, vol. 1, no. 4, pp. 606–617, Dec. 2007.
- [24] J. Huang and T. Zhang, "The benefit of group sparsity," Preprint 2009 [Online]. Available: arXiv:0901.2962
- [25] J. Peng, J. Zhu, A. Bergamaschi, W. Han, D. Y. Noh, J. R. Pollack, and P. Wang, "Regularized multivariate regression for identifying master predictors with application to integrative genomics study of breast cancer," *Ann. Appl. Stat.*, vol. 4, no. 1, pp. 53–77, 2010.
- [26] M. F. Duarte, W. U. Bajwa, and R. Calderbank, "The performance of group Lasso for linear regression of grouped variables Dept. Comput. Sci., Duke Univ., Durham, NC, USA, 2011, Tech. Rep. TR-2010-10.
- [27] E. Van Den Berg and M. P. Friedlander, "Theoretical and empirical results for recovery from multiple measurements," *IEEE Trans. Inf. Theory*, vol. 56, no. 5, pp. 2516–2527, May 2010.
- [28] J. Chen and X. Huo, "Theoretical results on sparse representations of multiple-measurement vectors," *IEEE Trans. Signal Process.*, vol. 54, no. 12, pp. 4634–4643, Dec. 2006.
- [29] Y. C. Eldar, P. Kuppinger, and H. Bolcskei, "Block-sparse signals: Uncertainty relations and efficient recovery," *IEEE Trans. Signal Process.*, vol. 58, no. 6, pp. 3042–3054, Jun. 2010.

- [30] X. Lv, G. Bi, and C. Wan, "The group Lasso for stable recovery of block-sparse signal representations," *IEEE Trans. Signal Process.*, vol. 59, no. 4, pp. 1371–1382, Apr. 2011.
- [31] M. Stojnic, F. Parvaresh, and B. Hassibi, "On the reconstruction of block-sparse signals with an optimal number of measurements," *IEEE Trans. Signal Process.*, vol. 57, no. 8, pp. 3075–3085, Aug. 2009.
- [32] M. Stojnic, " $\ell_2/\ell_1$ -optimization in block-sparse compressed sensing and its strong thresholds," *IEEE J. Sel. Topics Signal Process.*, vol. 4, no. 2, pp. 350–357, Apr. 2010.
- [33] M. Stojnic, "Block-length dependent thresholds in block-sparse compressed sensing," Preprint 2009 [Online]. Available: arXiv:0907.3679
- [34] S. Ji, D. Dunson, and L. Carin, "Multi-task compressive sensing," *IEEE Trans. Signal Process.*, vol. 57, no. 1, pp. 92–106, Jan. 2009.
- [35] S. Bakin, "Adaptive regression and model selection in data mining problems," Ph.D. dissertation, Australian National Univ., Canberra, A.C.T., Australia, 1999.
- [36] L. Meier, S. Van Den Geer, and P. Bühlmann, "The group Lasso for logistic regression," *J. Roy. Statist. Soc. Ser. B*, vol. 70, pt. 1, pp. 53–71, 2008.
- [37] M. Yuan and Y. Lin, "Model selection and estimation in regression with grouped variables," *J. Roy. Statist. Soc. Ser. B*, vol. 68, no. 1, pp. 49–67, 2006.
- [38] F. R. Bach, "Consistency of the group Lasso and multiple kernel learning," *J. Mach. Learn. Res.*, vol. 9, pp. 1179–1225, Jun. 2008.
- [39] Y. Nardi and A. Rinaldo, "On the asymptotic properties of the group Lasso estimator for linear models," *Electron. J. Statist.*, vol. 2, pp. 605–633, 2008.
- [40] K. Lounici, M. Pontil, A. B. Tsybakov, and S. van de Geer, "Taking advantage of sparsity in multi-task learning 2009 [Online]. Available: arXiv:0903.1468v1
- [41] D. Malioutov, M. Cetin, and A. S. Willsky, "A sparse signal reconstruction perspective for source localization with sensor arrays," *IEEE Trans. Signal Process.*, vol. 53, no. 8, pp. 3010–3022, Aug. 2005.
- [42] D. Needell and J. A. Tropp, "CoSaMP: Iterative signal recovery from incomplete and inaccurate samples," *Appl. Comput. Harmon. Anal.*, vol. 26, no. 3, pp. 301–321, 2008.
- [43] T. Blumensath and M. E. Davies, "How to use the iterative hard thresholding algorithm," presented at the Work. Struc. Parc. Rep. Adap. Signaux, 2009.
- [44] T. Blumensath and M. E. Davies, "Iterative hard thresholding for compressed sensing," *Appl. Comput. Harmon. Anal.*, vol. 27, no. 3, pp. 265–274, 2009.
- [45] D. L. Donoho, I. Drori, Y. Tsai, and J. L. Starck, "Sparse solution of underdetermined linear equations by stagewise orthogonal matching pursuit," Dept. Statist., Standard Univ., Standard, CA, USA, Tech. Rep., 2006.
- [46] M. Bayati and A. Montanari, "The Lasso risk for Gaussian matrices," 2011 [Online]. Available: arXiv:1008.2581v1
- [47] A. Maleki, "Approximate message passing algorithm for compressed sensing," Ph.D. dissertation, Stanford Univ., Stanford, CA, USA, 2011.
- [48] D. L. Donoho, A. Maleki, and A. Montanari, "Construction of message passing algorithms for compressed sensing," Preprint 2011.
- [49] M. J. Wainwright, G. Obozinski, and M. I. Jordan, "Support union recovery in high-dimensional multivariate regression," *Ann. Stat.*, vol. 39, pp. 1–47, 2011.
- [50] P. Schniter, "A message-passing receiver for BICM-OFDM over unknown clustered-sparse channels," *IEEE J. Sel. Topics Signal Process.*, vol. 5, no. 8, pp. 1462–1474, Dec. 2011.
- [51] P. Schniter, "Turbo reconstruction of structured sparse signals," in *Proc. IEEE Conf. Inf. Sci. Syst.*, Mar. 2010, pp. 1–6.
- [52] A. Fletcher, M. Unser, U. Kamilov, and S. Rangan, "Approximate message passing with consistent parameter estimation and applications to sparse learning," *IEEE Trans. Inf. Theory*, submitted for publication.
- [53] D. L. Donoho, I. M. Johnstone, and A. Montanari, *Accurate prediction of phase transition in compressed sensing via a connection to minimax denoising*, Nov. 2011.
- [54] R. G. Baraniuk, V. Cevher, M. F. Duarte, and C. Hegde, "Model-based compressive sensing," *IEEE Trans. Inf. Theory*, vol. 56, no. 4, pp. 1982–2001, Apr. 2010.
- [55] S. Jalali and A. Maleki, "Minimum complexity pursuit," in *Proc. Allerton Conf. Commun., Control, Comput.*, Sep. 2011, pp. 1764–1770.
- [56] D. L. Donoho, I. M. Johnstone, A. Maleki, and A. Montanari, "Compressed sensing over  $\ell_p$ -balls: Minimax mean square error," Preprint 2011 [Online]. Available: arXiv:1103.1943v2
- [57] Z. Yang and C. Zhang, "Sparsity-undersampling tradeoff of compressed sensing in the complex domain," in *Proc. IEEE Int. Conf. Acoust., Speech, Signal Process.*, 2011, pp. 3668–3671.
- [58] Z. Yang, C. Zhang, and L. Xie, "On phase transition of compressed sensing in the complex domain," *IEEE Signal Process. Lett.*, vol. 19, no. 1, pp. 47–50, Jan. 2012.
- [59] P. L. Combettes and V. R. Wajs, "Signal recovery by proximal forward-backward splitting," *SIAM J. Multiscale Model. Simul.*, vol. 4, no. 4, pp. 1168–1200, 2005.

**Arian Maleki** received his Ph.D. in electrical engineering from Stanford University in 2010. After spending 2011–2012 in the DSP group at Rice University, he joined Columbia University as an Assistant Professor of Statistics. His research interests include compressed sensing, statistics, machine learning, signal processing and optimization. He received his M.Sc. in statistics from Stanford University, and B.Sc. and M.Sc. both in electrical engineering from Sharif University of Technology.

**Laura Anitori** (S'09) received the M.Sc. degree (summa cum laude) in telecommunication engineering from the University of Pisa, Pisa, Italy, in 2005. From 2005 to 2007, she worked as a research assistant at the Telecommunication department, University of Twente, Enschede, The Netherlands on importance sampling and its application to STAP detectors. Since January 2007, she has been with the Radar Technology department at TNO, The Hague, The Netherlands. Her research interests include radar signal processing, FMCW and ground penetrating radar, and airborne surveillance systems. Currently, she is also working towards her Ph.D. degree in cooperation with the department of Geoscience and Remote Sensing at Delft University of Technology, Delft, The Netherlands on the topic of Compressive Sensing and its applications to radar detection. In 2012, she received the second prize at the IEEE Radar Conference for the best student paper award.

**Zai Yang** was born in Anhui Province, China, in 1986. He received the B.S. from mathematics and M.Sc. from applied mathematics in 2007 and 2009, respectively, from Sun Yat-sen (Zhongshan) University, China. He is currently pursuing the Ph.D. degree in electrical and electronic engineering at Nanyang Technological University, Singapore. His current research interests include compressed sensing and its applications to source localization and magnetic resonance imaging.

**Richard G. Baraniuk** (S'83–M'93–SM'98–F'02) received the B.Sc. degree in 1987 from the University of Manitoba (Canada), the M.Sc. degree in 1988 from the University of Wisconsin-Madison, and the Ph.D. degree in 1992 from the University of Illinois at Urbana-Champaign, all in Electrical Engineering. After spending 1992–1993 with the Signal Processing Laboratory of Ecole Normale Supérieure, in Lyon, France, he joined Rice University, where he is currently the Victor E. Cameron Professor of Electrical and Computer Engineering. His research interests lie in the area of signal processing and machine learning.

Dr. Baraniuk received a NATO postdoctoral fellowship from NSERC in 1992, the National Young Investigator award from the National Science Foundation in 1994, a Young Investigator Award from the Office of Naval Research in 1995, the Rosenbaum Fellowship from the Isaac Newton Institute of Cambridge University in 1998, the C. Holmes MacDonald National Outstanding Teaching Award from Eta Kappa Nu in 1999, the University of Illinois ECE Young Alumni Achievement Award in 2000, the Tech Museum Laureate Award from the Tech Museum of Innovation in 2006, the Wavelet Pioneer Award from SPIE in 2008, the Internet Pioneer Award from the Berkman Center for Internet and Society at Harvard Law School in 2008, the World Technology Network Education Award and IEEE Signal Processing Society Magazine Column Award in 2009, the IEEE-SPS Education Award in 2010, the WISE Education Award in 2011, and the SPIE Compressive Sampling Pioneer Award in 2012. In 2007, he was selected as one of Edutopia Magazine's Daring Dozen educators, and the Rice single-pixel compressive camera was selected by MIT Technology Review Magazine as a TR10 Top 10 Emerging Technology. He was elected a Fellow of the IEEE in 2001 and of AAAS in 2009.